https://doi.org/10.5194/egusphere-2025-2292
Preprint. Discussion started: 17 June 2025

Development and Validation of an Early Warning System for Coastal Flooding on a Mediterranean Urban Beach

Antonis Chatzipavlis[1], Daniele Trogu[2], Andrea Ruju[3], Juan Montes[4], Antonio Usai[2], Marco Porta[2], Giovanni Coco[5], Sandro De Muro[2], Paolo Ciavola[1]

[1] *Department of Physics and Earth Sciences, University of Ferrara, Via Saragat 1, 44122, Italy*
[2] *Department of Chemical and Geological Sciences, University of Cagliari, Monserrato, 09042, Italy*
[3] *Department of Civil, Environmental Engineering and Architecture, University of Cagliari, Via Marengo 2, 09123, Italy*
[4] *Earth Sciences Department, University of Cadiz INMAR, Avda. República Saharaui s/n, Puerto Real, 11510, Spain*
[5] *Faculty of Science, University of Auckland, Private Bag, 92019, New Zealand.*

Correspondence to: Antonis Chatzipavlis (antonis.chatzipavlis@unife.it)

Abstract. This study presents an Early Warning System (EWS) for coastal flooding that integrates wind, wave, and sea level forecasts which are validated using *in-situ* records. The system employs the SWAN spectral wave model to simulate nearshore hydrodynamics while an empirical approach is used to assess Total Watel Level (TWL) exceedances over a user-defined morphological threshold, deriving from analytical topographic surveys. This approach utilizes six widely used empirical methods for wave run-up estimation and makes use of the most effective one after calibration. The performance of the EWS is assessed through six monitored flood events of varying magnitude and hydrodynamic conditions, demonstrating strong agreement between projected TWL exceedances and observed flooding occurrences, particularly under high-energy wave conditions. Minor discrepancies are noted during events with marginal TWL exceedances over short durations. Results underscore the system's potential as a valuable tool for coastal hazard assessment and risk management, with future improvements focusing on dynamic updates of the beach morphology and the integration of suitable machine learning algorithms.

1. Introduction

Coastal floods are considered among the most hazardous natural disasters, posing significant threats to coastal communities, affecting livelihood and crucial socio-economic aspects. Millions of people living in coastal areas are currently at risk of displacement due to flooding, leading to the loss of livelihoods, social disruption and economic costs related to relocation (Neumann et al., 2015a; Hauer et al., 2016; Nicholls et al., 2019; IPCC, 2023). At the same time, critical infrastructure assets such as ports, coastal airports, power plants and transportation networks are particularly vulnerable, with potential repair and adaptation costs running into tens of billions of dollars annually (Neumann et al., 2015b; UNCTAD, 2018; Monioudi et al., 2018; Asariotis et al., 2024). In addition, coastal flooding risks devalue properties in flood-prone areas, potentially leading to losses in property value worth billions of dollars (Murfin and Spiegel, 2020; Vousdoukas et al., 2020; Bakkensen and Barrage,

https://doi.org/10.5194/egusphere-2025-2292
Preprint. Discussion started: 17 June 2025

2021). The economic impacts of coastal flooding are expected to rise, as sea levels are increasing at an accelerating rate. Global mean sea level has risen by about 0.2 m since 1900, with a significant acceleration in recent decades (Jevrejeva et al., 2016; IPCC, 2023). Future projections indicate that Mean Sea Level (MSL) could rise by 0.4 - 0.8 m by 2100, depending on emissions scenario, significantly heightening the risk of coastal flooding (IPCC, 2023). Extreme Sea Level (ESL) events occurring during extreme storms/surges due to the increased hydrodynamic action are additionally expected to increase over the 21st century (Vousdoukas et al., 2018a; Almar et al., 2021). The combination of higher MSL and ESL can lead to more frequent and severe coastal inundation events, making previously safe areas susceptible to flooding necessitating substantial investments in mitigation and adaptation strategies to protect vulnerable coastal communities (Vousdoukas et al., 2018a; IPCC, 2023).

Consequently, there is an urgent need for decision-support tools to assist local stakeholders and coastal planners. In the long run, such tools can be used to effectively design risk-reduction strategies based on future flood risk projections. In the short-term, the development of Early Warning Systems (EWSs) plays a crucial role in safeguarding coastal areas. Several EWSs for coastal flooding have been developed to enhance the resilience of coastal communities (e.g. Harley et al., 2012; Stokes et al., 2021; Le Gal et al., 2023; Sanchez-Artus et al., 2025). These systems integrate hydrodynamic modeling, real-time monitoring networks, and forecasting techniques to predict and mitigate flood impacts on a large (national/regional) or localized scale. Large scale operating EWSs cover broader geographical areas, averaging out specific local conditions. On the other hand, locally tailored systems provide highly specific and customized warnings, using real-time monitoring and detailed modeling of nearshore hydrodynamics at finer resolution.

At a national scale, one of the earliest efforts for the prediction of storm surge induced flooding during hurricane activity is the Sea, Lake, and Overland Surges from Hurricanes (SLOSH) model developed by the U.S. National Oceanic and Atmospheric Administration (NOAA) that integrates coastal topo-bathymetry, meteorological data and tide conditions (Jelesnianski et al., 1992), providing crucial data for early warning and evacuation planning. Furthermore, Xiao et al. (2006) introduced the Coastal and Estuarine Storm Tide (CEST), a numerical modeling system that integrates multiple data sources, such as tidal predictions, meteorological data, and wave information to predict water levels during extreme weather events. In the United Kingdom, the Joint Met Office - Environment Agency Flood Forecasting Centre (FFC) utilizes an EWS that integrates meteorological and hydrological data to deliver timely flood risk assessments across the United Kingdom (Stephens and Cloke, 2014). More recently, the European Coastal Flood Awareness System (ECFAS) generated real-time flood forecasts using pre-identified local morphological thresholds at defined coastal sectors along the entire European coastline, together with a combination of predicted hydrodynamic conditions and high-resolution numerical modeling (LISFLOOD-FP) suited to regional-to-local scale assessments (Le Gal et al., 2023). Locally tailored systems offer customizable early warning solutions by integrating multiple datasets and real-time hydrodynamic modeling of the nearshore processes at finer scales. For instance, a fully operational EWS operates at the region of Emilia-Romagna (Italy) that integrates atmospheric, hydrodynamic, and morphodynamic models to provide three-day forecasts of dune erosion and marine flooding at strategic locations, translating model outputs into actionable information for emergency planners (Ciavola et al., 2011; Armaroli et al., 2012; Harley et al., 2012). Furthermore, Biolchi et al. (2022) presented the integration of ensemble prediction methods into a coastal EWS that employs an advanced

https://doi.org/10.5194/egusphere-2025-2292
Preprint. Discussion started: 17 June 2025

morphodynamic model (XBeach – Roelvink et al., 2009) for selected cross-shore sections of Emilia-Romagna. Sanchez-Artus et al. (2025) presented a high-resolution hydrodynamic operational service using the XBeach model to forecast coastal flooding for three urban beaches in Barcelona (Spain). Garzon et al. (2023) introduced a Bayesian networks-based EWS for wave-induced flooding that makes use of a probabilistic approach to assess the flooding likelihood, accounting for multiple uncertain variables, including wind, wave and tide conditions. In Venice lagoon, the "Acqua Alta" (high water) surge forecast system demonstrates the effective integration of a hydrodynamic model used for sea level forecasts and an Artificial Neural Network (ANN) module used to correct the modeled output with observed sea level data in the Adriatic Sea (Bajo and Umgiesser, 2010; Zampato et al., 2016). The most recent development in coastal flood forecasting is the exclusive use of ANNs that integrate atmospheric (wind and barometric pressure) and hydrodynamic (waves, sea level and tide) parameters to generate acceptable sea level predictions. Several studies have tested different ANNs at various locations worldwide, found to be capable of providing water level predictions during extreme surge events with RMSEs ranging between 9 - 34 cm, depending on the event's magnitude and duration (Hashemi et al., 2016; Wang et al., 2016; Wang and Yuan, 2018; Chao et al., 2020; Dato et al., 2024).In Venice lagoon, the "Acqua Alta" (high water) surge forecast system demonstrates the effective integration of dynamic and neural network models, providing accurate forecasts of storm surge events in Venice Lagoon, enabling authorities to implement timely interventions (Bajo and Umgiesser, 2010). A more recent development in coastal flood forecasting is the Bayesian networks-based EWS for wave-induced flooding, as proposed by Garzon et al. (2023). This system uses a probabilistic approach to assess the likelihood of wave-induced flooding, accounting for multiple uncertain variables, including wind, wave and tide conditions.

To trigger the warning levels, it is essential to establish thresholds based on the predicted intensity of the flood event. Defining these thresholds and identifying extreme levels can be carried out by employing the TWL at the coastal boundary. TWL at a given time (t) can be defined by synthesizing three different components as (Pugh, 1987): $TWL(t) = Zo(t) + T(t) + R(t)$, where Zo (t) is the mean sea level due to atmospheric forcing (pressure and wind, non-tidal residual), T(t) is the tidal component and R(t) is the wave run-up expressed as the sum of level changes due to wave set-up and the swash. Over recent years, a number of studies have suggested different approaches for the calculation of the non-tidal residuals (R(t) and Zo(t)). Vousdoukas et al. (2016), Vousdoukas et al. (2018b) and Le Gal et al. (2023) estimate TWL as the sum of the mean sea level (Zo(t)), the tidal signal (T(t)) and the wave set-up to predict the extension of coastal flooding. Del Rio et al. (2012) proposed a method for TWL calculation that involves the tidal signal, the wind-induced setup, barometric pressure changes and sea level perturbations due to wave action, whereas Jimenez et al. (2009) used wave information for estimating the inundation danger of the coast of Emilia-Romagna region (Italy), Catalan (Spain) and Languedoc-Rossillon (France) coastlines. On the other hand, Rulent et al. (2020), Caruso and Marani (2022) and Croteau et al. (2023) use a more simplistic approach, where TWL is estimated as the sum of the mean sea level, tide and level variations associated with storm surges, excluding the wave induced perturbations.

During storms or elevated tide and surge conditions wave run-up can significantly exceed the elevation of coastal protection elements (like dunes and seawalls) leading to overwash and flooding. However, wave run-up processes are not frequently

https://doi.org/10.5194/egusphere-2025-2292
Preprint. Discussion started: 17 June 2025

integrated into EWSs due to the limited availability of high-resolution coastal topo-bathymetry, as well as the complexity of simulating the highly dispersive wave transformation at the nearshore (e.g. Ardhuin et al., 2009; Naeini and Snaiki, 2024). Even so, the numerical models capable to resolve such non-linearities and provide sufficient wave run-up estimates require significant computational time and effort (e.g. XBeach - Roelvink et al, 2009; SWASH - Zijlema et al., 2011; Boussinesq based model - Klonaris et al., 2013). Thus, coastal scientists and engineers commonly use parameterized empirical expressions that have been found capable in providing realistic estimates, in different beach environments (e.g. Ruggiero et al. 2004; Stockdon et al., 2006; Vousdoukas et al., 2009; Senechal et al., 2011; Paprotny et al., 2014; Suanez et al., 2016; Poate er al., 2016; Gomes da Silva et al., 2020; Bujak et al., 2023).

In this context, the aim of the present contribution is to report the development and validation of an operational flood EWS (henceforth called NEPTUNE-EWS) that has been configured and tested on a microtidal wave-dominated beach in the southern part of Sardinia Island (Italy). The system utilizes high-resolution topo-bathymetric data and locally generated wind-wave forecasts to simulate nearshore hydrodynamics and predict the Total Water Level (TWL), incorporating wave run-up estimates. Flood forecasts are based on the exceedance of TWL over predefined morphological thresholds, which are dynamically updated through repeated topographic leveling at selected locations. The system's performance is evaluated against six overwash and flood events of varying magnitude, triggered by different wind-wave conditions, and monitored in real time through an autonomous video monitoring system.

2. Methodology

2.1 Pilot Site: Poetto beach

Poetto is an urban microtidal (maximum tidal range of 40 cm during spring cycles and 20 cm during neap cycles, Biondo et al., 2020), wave dominated beach fronting the city of Cagliari, hosting about 100,000 people per day during the summer season, making it the most visited beach of Sardinia (Strazzera et al., 2008). The high carrying capacity of Poetto is justified by its dimensions (length of about 8 km and maximum width of about 100 m), whereas a significant number of coastal facilities and assets can be found at the low-lying (maximum elevation of about 2.5 m above sea level) backshore coastal promenade. Due to its socio-economic and environmental importance for the region, the Mediterranean Geomorphological Coastal and Marine Laboratory (MedCoastLab) of the University of Cagliari developed a monitoring program that involves analytical studies of Poetto's hydro-morphodynamics, making it one of the most studied beaches of Sardinia (e.g. De Muro et al., 2017; Ruju et al., 2019; Biondo et al., 2020; Ruju et al., 2022; Trogu et al., 2023; Trogu et al., 2024).

Poetto can be considered as an intermediate beach having mild to intermediate foreshore slopes ($\tan\beta$) that range between 0.07 - 0.15, backed by a relatively narrow (between 10 - 50 m) and low (maximum elevation at 2.2 m above sea level) primary dune system (Ruju et al., 2022). Its low-lying topography makes the beach vulnerable to flood and erosion phenomena during events of increased hydrodynamic action. As an effort to limit erosion, a beach nourishment project (of about 300,000 m^3 of sand) was carried out in 2002 at the Western sector, significantly modifying the textural, compositional and morphological features

https://doi.org/10.5194/egusphere-2025-2292
Preprint. Discussion started: 17 June 2025

of the beach (De Muro et al., 2017). Most of the coarser bioclastic material used for nourishment was rapidly eroded in the following years with a registered erosion rate of up to 3 m/year in the Western, most urbanized and vulnerable sector (Biondo et al., 2020). During autumn - early winter periods, the foreshore beach is periodically covered by *Posidonia oceanica* banquettes or/and accumulation of *Arundo donax* reeds as a response to increased hydrodynamic activity and the species biological cycle (Ruju et al., 2022; Trogu et al., 2023). As a combined result of the wave action and the elevated level during storm surges, Poetto emerged beach is periodically flooded by Southeast storms, with a flooding extension that episodically reaches the coastal promenade of the western most vulnerable beach sector (De Muro et al., 2017; Trogu et al., 2024).

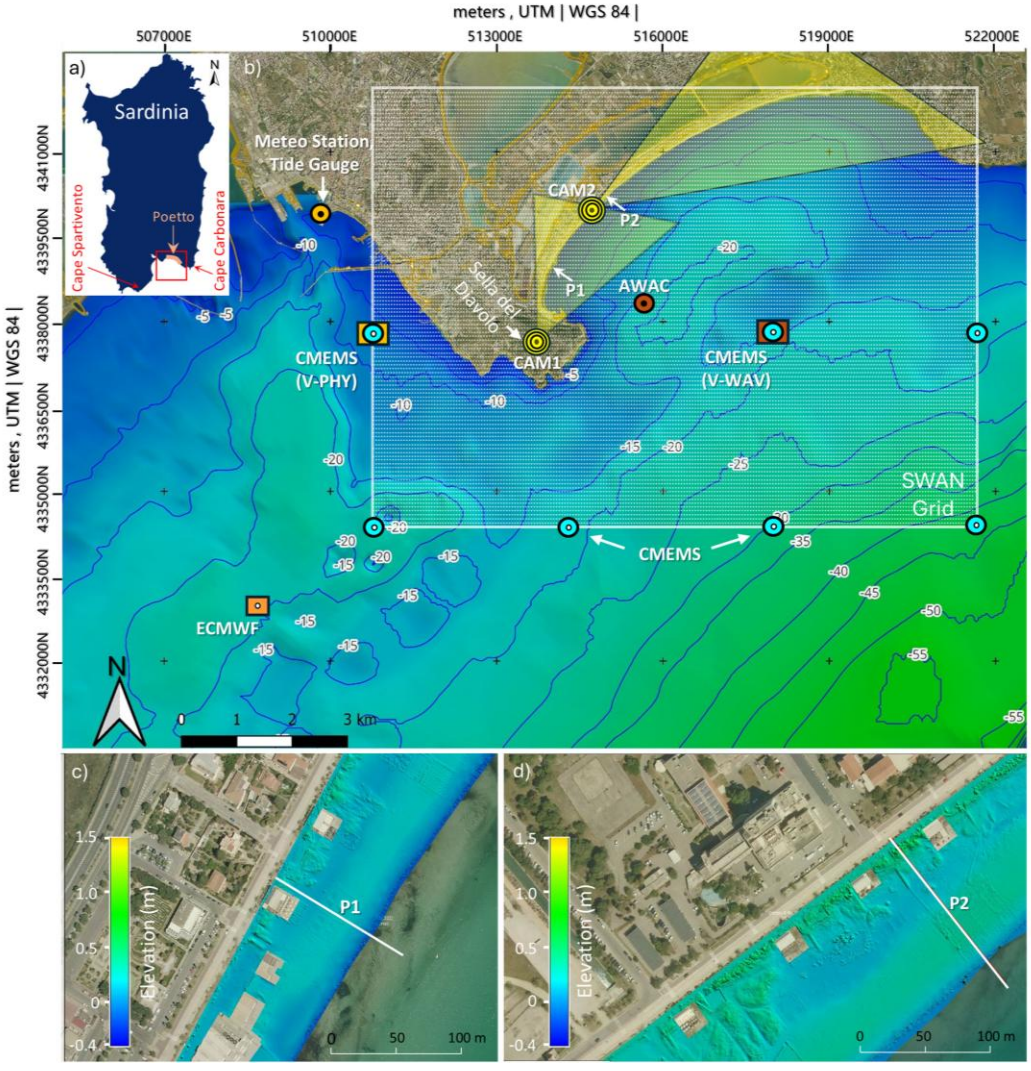

Figure 1: a) Map of Sardinia showing the location of Poetto beach. b) Bathymetry of the wider area of Poetto and Cagliari port. The locations of the coastal videocameras and their fields of view, cross-shore profiles P1 and P2, AWAC logger, meteorological station and tide gauge, CMEMS and ECMWF grid points, and the computational grid used in SWAN, are also shown. b) and c) Elevation maps (above MSL) of the locations close to cross-shore profiles P1 and P2 (Image source: Sardegna Geoportale, 2024).

https://doi.org/10.5194/egusphere-2025-2292
Preprint. Discussion started: 17 June 2025

A coastal video monitoring system is deployed in Poetto, set to monitor the western and central sectors of the beach (proximal beach stretch of about 2.7 km - see Fig. 1b). The system consists of two videocameras that provide optical records (frames) of high frequency (4 Hz) and time coverage (for 20 minutes, at the beginning of every three hours during daylight), used for the detection of overwash and flooding events, amongst other hydro-morphological parameters (for details see Trogu et al., 2023). For the context of this work, the performance of NEPTUNE-EWS is assessed through a selected timeseries of six overwash (i.e. limited water coverage or/and *Posidonia oceanica* traces) and flooding (i.e. extended water coverage) events of different characteristics, which have been monitored/recorded by the coastal videocameras (see also Section 3.2).

2.2 NEPTUNE-EWS: Structure and Computational Elements

The NEPTUNE-EWS is set-up on the web-server of the MedCoastLab, implemented as Linux shell scripts that call dedicated Python functions/scripts. The system is fully operational providing forecasts of the Total Water Level (TWL) values for the next 4 days with a 3-hour timestep. NEPTUNE-EWS is fed with a detailed bathymetric Digital Elevation Model (DEM), coupled with analytical survey data (topographic DEM) to detect low elevation and prone to flood areas, according to historical flood/overwash records derived from the coastal video monitoring system. For these areas two crucial morphological parameters (the foreshore (wet) slope (tanβ) and the berm height (B)), are extracted from the topographic data. Foreshore slope is a key parameter that controls wave run-up, which is a main component for estimating Total Water Level (TWL) (see Section 2.2.4). Berm height is used as an exceedance threshold against the projected TWL, to assess flood risk at the examined locations. The system's structure and the main computational elements are presented in Figure 2.

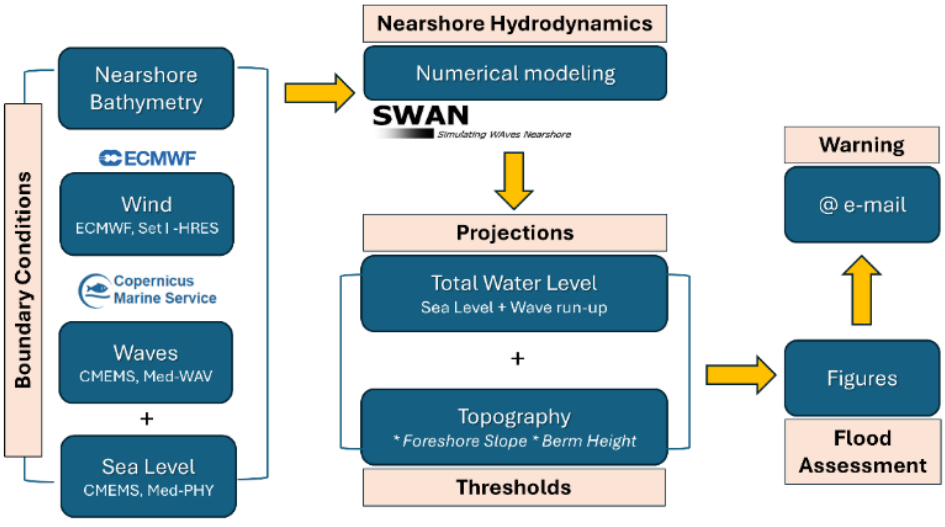

Figure 2: Structure of the NEPTUNE-EWS.

https://doi.org/10.5194/egusphere-2025-2292
Preprint. Discussion started: 17 June 2025

During execution of NEPTUNE-EWS, the initial step involves the extraction of the wind and hydrodynamic forecasts from a local area weather model. More specifically, hourly forecasts of i) the wind conditions (two horizontal velocity components, u10 and v10); ii) the wave climate (13 parameters) involving the significant wave heights, spectral moments/peak periods and mean directions of both wind generated and swell (primary and secondary) wave components; and iii) the sea level perturbations due to the combined action of the tidal cycle and barometric perturbations, are extracted from widely used e-databases (Table 1). Wind forecasts are provided by the European Center for Medium-range Weather Forecasts (ECMWF), whereas wave and sea level forecasts are extracted from the Copernicus Marine Environmental Monitoring Service (CMEMS) virtual buoys/e-database using the Copernicus Marine Toolbox - version 2.0.0 (CMS, 2025). The forecasted wind-wave climate deriving from the ECMWF and CMEMS e-databases, is used as input to the SWAN (Simulating WAves Nearshore) model (e.g. Zijlema and van der Westhuysen, 2005). The computational elements of NEPTUNE-EWS are reported in the following sections. Section 2.2.1. presents the boundary conditions and the thresholds used during initial system set-up, whereas the process of simulating nearshore hydrodynamics and TWL estimates are presented in Section 2.2.2.

2.2.1 Boundary conditions

Topography and Bathymetry

Nearshore bathymetry was retrieved on 21/05/2019 with the use of a boat equipped with a single beam echosounder (Reson Navisound 215) combined with a DGPS Differential Global Positioning System (DGPS - Omnistar 8300HP), set to operate at 5 Hz and interfaced through a notebook via the dedicated Reson PDS2000 navigation and acquisition software. The boat navigated through dense (spaced at about 350 m) cross- and long-shore transects from shallow depths (of about 1 m) up to the inshore expansion limit of the *Posidonia oceanica* meadow at depths between 10 - 18 m. The EMODnet bathymetric database (EMODnet, 2024) integrated the retrieved high-resolution bathymetry to provide the complete nearshore DEM (up to about 40 m). Furthermore, an Unmanned Aerial Vehicle (Enac-certified DJI Phantom 4 Pro APRs with GSD= 3/5 cm per pixel) was used to obtain a detailed topographic DTM (Digital Terrain Model) on 22/05/2019.

In addition, eight topographic surveys were carried out during the period 2017 - 2024 along the two most prone to flooding locations/cross-shore profiles (named P1 and P2) according to the topographic DEM and the camera records. The topographic data were measured with the use of a Real Time Kinematic Differential Global Positioning System (RTK-DGPS), collecting survey points from the dune system till shallow depths of about 1 m.

Meteorology and Hydrodynamics

Wind forecast is extracted from the ECMWF's dataset (Table 1 - ECMWF, 2025). The dataset is based on the Set I - High RESolution (HRES) atmospheric model, specifically tailored to compute wind components at 10 m height (u10 and v10) for 10 days ahead, updated twice a day, with a spatial resolution of 0.1° x 0.1° (of about 9 km) and hourly frequency. The operational implementation of ECMWF Set I-HRES benefits from improvements in computational methods and the integration

https://doi.org/10.5194/egusphere-2025-2292
Preprint. Discussion started: 17 June 2025

of observational data (Herschbach et al., 2020). To validate the accuracy of ECMWF forecasts in Poetto, the forecasted wind climate is compared against wind records of a meteorological station installed and operating at the port of Cagliari at an elevation of 3 m, with a recording frequency of 10 minutes (see Fig. 1b). The data are accessible through the monitoring network of the Italian Institute for Environmental Protection and Research (ISPRA) (ISPRA, 2025). To achieve that, wind data from the closest available geographical point of the ECMWF database were used (located at a distance of 7.2 km offshore the meteorological station - see Fig. 1b). For comparison, wind records of the meteorological station were extracted for the same timestep with the ECMWF forecasts (hourly) and were converted to wind velocity at 10 m height (U10) as $U10 = Uz\,(10/z)^{1/7}$, $0 < z < 20$, where z, is the elevation of the meteorological station (USACE, 1984). Furthermore, the effective wind events (i.e. storms with intensity greater than 4 Beaufort, blowing from directions within the effective fetch of Poetto) were isolated by using the criterion of Sanchez-Arcilla et al. (2008), according to which a wind event can be classified as storm surge if it has a duration of at least 6 hours, while any break in strong winds (in this case greater than 4 Beaufort) should not exceed 18 hours between consecutive wind records. These events were compared against the wave heights projected by CMEMS to identify trends and assess the wind-generated waves during increased wind activity (see Section 3.1).

Table 1: Wind, wave and sea level forcing parameters as extracted/used by NEPTUNE-EWS to simulate coastal hydrodynamics. The CMEMS Med-WAV re-analysis product used for validation of the wave climate is also reported.

Source	Database	Product ID	Extracted Parameters (as listed)
ECMWF, Set I -HRES (ECMWF, 2025)	Atmospheric fields - single level – forecast HRES	SET I-i-a	'10U': Wind velocity, horizontal component - u
			'10V': Wind velocity, horizontal component - v
CMEMS, Med-PHY (Clementi et al., 2021)	*MEDSEA_ANALYSIS_FORECAST_PHY_006_013*	*cmems_mod_med_phy_ssh_anfc_4.2km-2D_PT1H-m*	'ZOS': Sea surface elevation (Tide included)
CMEMS, Med-WAV (forecasts) (Korres et al., 2023)	*MEDSEA_ANALYSIS_FORECAST_WAV_006_017*	*cmems_mod_med_wav_anfc_4.2km_PT1H-i*	'VHM0': Spectral significant wave height
			'VMDR': Mean wave direction (from)
			'VTPK': Peak wave period
			'VTM02': Spectral moments (0,2) wave period
			'VHM0_WW': Spectral significant wind wave height
			'VMDR_WW': Mean wind wave direction (from)
			'VTM01_WW': Spectral moments (0,1) wind wave period
CMEMS, Med-WAV (re-analysis) (Korres et al., 2021)	*MEDSEA_MULTIYEAR_WAV_006_012*	*med-hcmr-wav-rean-h*	'VHM0_SW1': Spectral significant primary swell wave height
			'VMDR_SW1': Mean primary swell wave direction (from)
			'VTM01_SW1': Spectral moments (0,1) primary swell wave period
			'VHM0_SW2': Spectral significant secondary swell wave height
			'VMDR_SW2': Mean secondary swell wave dir. (from)
			'VTM01_SW2': Spectral moments (0,1) secondary swell wave period

https://doi.org/10.5194/egusphere-2025-2292
Preprint. Discussion started: 17 June 2025

Wave climate forecast is extracted from the CMEMS download center through the wave component of the Mediterranean forecasting system (Med-WAV) (Table 1 - Korres et al., 2023). Forecasts are based on the WAM6 numerical model, developed from the fundamental work of Hasselmann et al. (1973). WAM6 is one-way nested, designed to simulate ocean wave dynamics with a spatial resolution of 1/24º (of about 4.2 km) and high precision. The model resolves the prognostic part of the wave spectrum with 24 directionally and 32 logarithmically distributed frequency bins, whereas the solutions are corrected by an optimal interpolation data assimilation scheme of along track satellite observations of the significant wave height (Oikonomou et al., 2023). The model is updated twice a day and provides hourly forecasts for 10 days ahead of the main wave parameters (significant wave height, mean/peak wave period and mean direction) for a wind generated wave component and two swell wave components (primary and secondary). The performance of Med-WAV was assessed against the closest available records of an AWAC *(*Acoustic Wave And Current) profiler deployed for a 45-day period between 16/10/2020 - 30/11/2020 at 18 m depth, distanced 2.1 km away from the most proximal CMEMS point/virtual buoy (CMEMS V-WAV) located at a similar depth (see Fig. 1b). The reanalysis dataset used for comparison is generated from the WAM4 (version 4.6.2) model (Table 1 - Korres et al., 2021), as the latest WAM6 based forecasts became available at a later stage (since 01/12/2021).

Sea Surface Height (SSH) forecast is similarly extracted from CMEMS download center through the physical component of the Mediterranean forecasting system (Med-PHY) (Table 1 - Clementi et al., 2021). Med-PHY provide hourly forecasts of the SSH perturbations (parameter zos), considering both the barometric component and the tidal signal. To achieve that, it utilizes a coupled hydrodynamic-wave model (NEMO and WAVEWATCH III) to account for wave-current interactions, while it integrates observational data through a 3D variational data assimilation scheme known as OceanVar (CMS, 2024).

The accuracy of the modeled wind, wave and sea level parameters provided by ECMWF and CMEMS was evaluated against the *in-situ* measurements from a tide gauge operating in Cagliari port, at a location next to the meteorological station as part of the Italian tide gauge network (ISPRA, 2025). These data were plotted against the timeseries deriving from the closest to this location CMEMS virtual buoy, at a distance of 2.6 km away (CMEMS V-PHY, see Fig. 1b).The comparison is carried out using a set of statistical indicators that involve the Correlation coefficient (R), Mean Absolute Error (MAE), Scaled Mean Absolute Error (SMAE), Mean Residual (Bias) and Root Mean Square Error (RMSE).

2.2.2 Simulations of nearshore hydrodynamics, TWL forecasts

The projected wind-wave climate deriving from the ECMWF and CMEMS and the detailed nearshore bathymetry are set as input to the SWAN model. SWAN is a spectral wave model based on the wave action balance (e.g. Stokes et al., 2021). The grid used in SWAN has a spatial resolution of 0.001° (of about 100 m - see Fig. 1b), allowing the representation of the main wave transformation processes. Reconstruction of the wave spectra is based on the approach of Ruju et al. (2022) who investigated nearshore wave spreading in Poetto beach (with the use of the same grid as currently available in NEPTUNE-EWS) and validated SWAN's wave forecasts against *in-situ* wave records of an AWAC. This approach is also consistent with Ruju and Viola 2024 who suggested that, during multimodal wave conditions, nearshore wave predictions can be improved by

https://doi.org/10.5194/egusphere-2025-2292
Preprint. Discussion started: 17 June 2025

using boundary conditions in which wave spectra are reconstructed from partitioned wave parameters rather than from bulk integrated wave parameters.

The intensity of the flood event is assessed through identifying TWL thresholds. This is achieved by synthesizing the three TWL components (Zo, T and R – Pugh, 1987). Wave run-up contribution to the TWL (R) is determined from the spectral wave parameters (Significant wave height - Hs and peak wave period - Tp) computed by SWAN outside the surf zone along the selected, prone to flood locations transects (in this case, P1 and P2). The system uses the spectral wave parameters to estimate the offshore wave parameters (Ho) and length (Lo), with the use of an inverse shoaling function as $L_o = gT_p^{\,2}/2\pi$ and $H_o = H_s/k_s$. Where g, is the gravitational acceleration (9.81 ms^{-1}) and k_s, is the shoaling coefficient calculated as $\sqrt{cg_0/cg}$. Where cg_0 is the offshore group velocity and cg the nearshore (shallow) group velocity. Offshore group velocity is calculated as $c_0/2$, where c_0 is the offshore wave celerity calculated as the ratio of Lo/Tp . Nearshore group velocity is calculated as c·n, where c, is the wave celerity equal to L/Tp and n, the group velocity factor accounting for dispersion effects in finite depth.

Table 2: The empirical formulae for wave run-up estimates employed in NEPTUNE-EWS.

Equation	Type	Source
$R_{max} = a \cdot H_o\xi = k \cdot tan\beta(H_0L_0)^{0.5}$	Impermeable Structures	Hunt (1959)
$R_{2\%} = (0.83\xi + 0.2)H_o$	Reflective	Holman (1986)
$R_{max} = 0.12H_o/\,(H_o/L_o)^{0.5}$	Reflective	Douglas (1992)
$R_{max} = b \cdot H_0(g/2\pi)^{0.5}$	Mildly Sloped - Open Sea	Nielsen and Hanslow (1991)
$R_{2\%} = c \cdot \xi \cdot H_0$	Dissipative	Ruggiero et al. (2004)
$R_{2\%} = 1.1\left(0.35\tan\beta(H_0L_0)^{0.5} + \frac{[H_0L_0(0.563\tan\beta^2 + 0.004)]^{0.5}}{2}\right)$	Intermediate & Reflective ($\xi \geq 0.3$)	Stockdon et al., (2006)
$R_{2\%} = 0.043(H_0L_0)^{0.5}$	Dissipative ($\xi < 0.3$)	
Parameters		
$\xi = \frac{tan\beta}{(H_0/L_0)^{0.5}}$	Iribarren Number	Iribarren and Nogales, 1949
a, empirical coefficient ranging between 2.3 - 3.0 (average waves - storm conditions)	-	Hunt (1959)
b, empirical coefficient typically ranging between 0.6 - 0.8	-	Nielsen and Hanslow (1991)
c, empirical coefficient ranging between 0.5 - 1.1	-	Ruggiero et al. (2004)
tanβ - foreshore slope (wet)	-	
Ho, offshore wave height	-	
Lo, offshore wave length	-	

After estimation of the offshore wave parameters, six commonly used empirical expressions controlled by the incident wave energy and the foreshore slope are employed by NEPTUNE-EWS (Table 2). The performance of each formula is assessed

https://doi.org/10.5194/egusphere-2025-2292
Preprint. Discussion started: 17 June 2025

against the overwash and flooding events of different duration and magnitude (monitored by the coastal videocameras) to select the most effective (see also Section 3.2).

3. Results

3.1 Topographic Records

Specific morphodynamic patterns are evident when investigating the evolution of P1 and P2 profiles during the last 7-year period (Fig. 3). First, both locations experienced substantial losses in dune and berm heights. More specifically, location P2 experienced dune and berm elevation changes by 0.9 m and 0.4 m, respectively compared to 2017 (Table 3). Such changes are of great importance for setting the morphological threshold of NEPTUNE-EWS (in this case the berm height).

In 2020 the berm height was higher than 2017, which may be attributed to the sedimentation of reeds, which were found to be transported at the beach during this period (see Trogu et al., 2023). It also has to be noted that the position of the shoreline in this location is found to have accreted by 3.6 m in 2024, compared to 2017. Profile P1 is found to be the most vulnerable location in terms of shoreline erosion with recorded retreat of 23.3 m during the examined period. Nevertheless, during the last survey (18/10/2024) it was found that shoreline position has been accreted by 9 m compared to the 20/06/2024 records. The latter is linked with the technical works (bulldozing for beach flattening) that took place during this period. Moreover, during the same period both height and width of the foreshore berm were found to decrease by 0.4 m and 15.1 m, respectively (Fig. 3). Dune height in this location has progressively decreased from 2.01 m in 2017 to 1.67 m in 2024 (elevation loss rate of about 5 cm per annum), being however stabilized on its width.

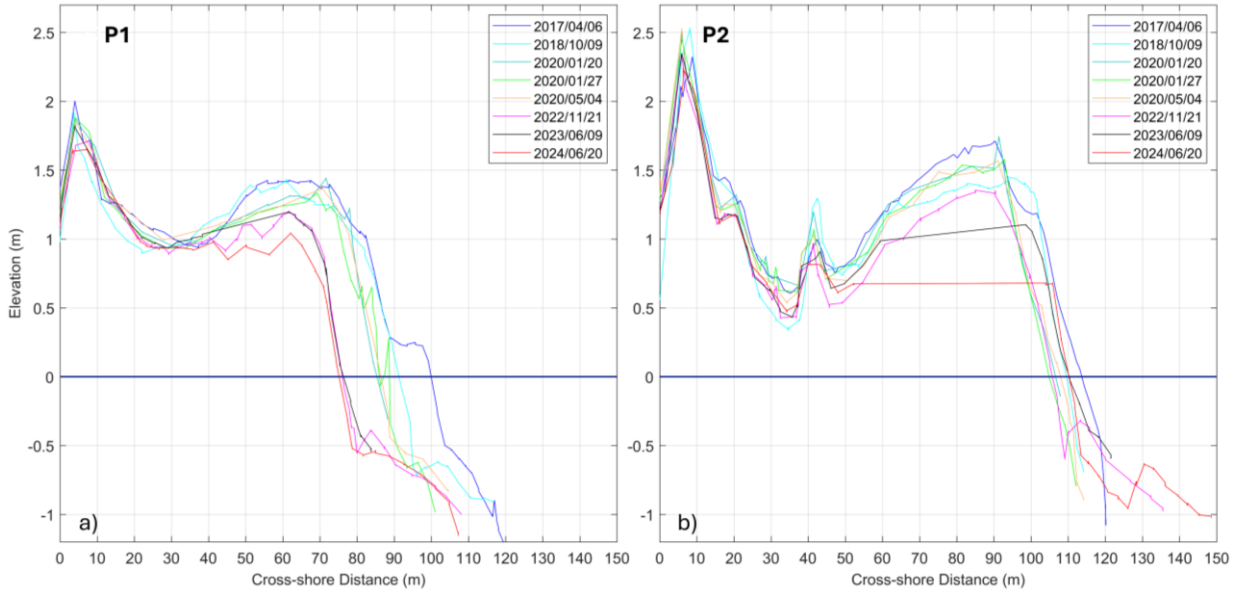

Figure 3: Evolution of cross-shore profiles a) P1; and b) P2 during the period 2017-2024.

https://doi.org/10.5194/egusphere-2025-2292
Preprint. Discussion started: 17 June 2025

Despite the changes in beach width and berm height, the foreshore slope (tanβ) for cross-shore profiles P1 and P2 is relatively constant, ranging between 0.10 – 0.12 and 0.07 – 0.08, respectively (Table 3). Berm height is commonly used as the threshold for coastal flooding. As berm height changes over time, the most updated values deriving from field measurements are used as flooding threshold values in NEPTUNE-EWS, considering also the seasonal cross-shore berm differentiations (i.e. summer - winter berm deposition).

Table 3: Morphological parameters of Poetto beach at cross-shore profiles P1 and P2 as obtained from the nine topographic surveys conducted during the period 2017-2024.

Survey Date (yy/mm/dd)	Dune Height (m)		Berm Height (m)		Foreshore Slope (tanβ)	
	P1	P2	P1	P2	P1	P2
2017/04/06	2.01	3.22	1.44	1.71	0.11	0.07
2018/10/09	1.92	2.55	1.45	1.42	0.12	0.08
2020/01/20	1.87	2.52	1.44	1.74	0.11	0.07
2020/01/27	1.88	2.51	1.33	1.58	0.11	0.08
2020/05/04	1.86	2.47	1.38	1.56	0.12	0.07
2022/11/21	1.82	2.45	1.20	1.57	0.11	0.07
2023/06/09	1.71	2.34	1.19	1.35	0.12	0.07
2024/06/20	1.67	2.23	1.05	1.11	0.11	0.07

3.2 Validation of forecasts

3.2.1 Wind regime

The majority of the wind records (74%) deriving from the meteorological station are found to blow mainly from NW and NNW directions, while 14% had intensity greater than 4 Beaufort ($U_{10} > 8$ ms^{-1}) (Fig. 4). Generated winds within the directional range of the effective fetch of Poetto (i.e. between 117° - 202°), are found to represent 22% of total records. Interestingly, 10% of the recorded wind had velocities greater than 4 Bf, capable of locally generating wind waves. The respective forecasted ECMWF, SET I-HRES U_{10} timeseries are found to align well with the *in-situ* records following similar trends, both in velocity and direction. Nevertheless, the intensity of the ECMWF forecasted winds blowing from directions within the effective fetch of Poetto, are found to be slightly lower (of about 2 - 3 ms^{-1}). The latter is also evident when examining the timeseries of both, recorded and forecasted wind climate (Fig. 4).

https://doi.org/10.5194/egusphere-2025-2292
Preprint. Discussion started: 17 June 2025

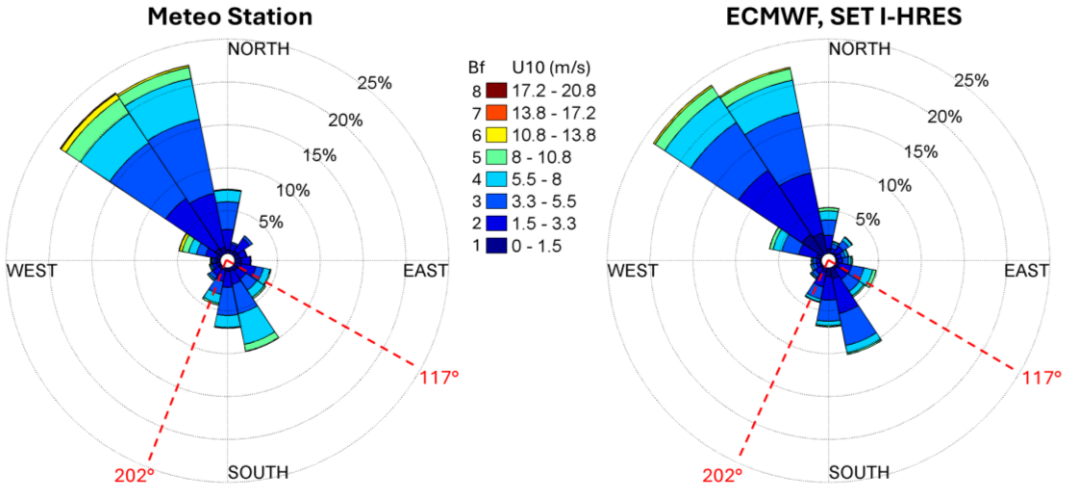

Figure 4: Recorded (left) and forecasted (right) wind roses. The dashed red lines denote the directional limits of the effective fetch of Poetto beach.

The smoothed timeseries (window size equal to 200) of both recorded and forecasted wind climate follow similar patterns with slight differences (of about 0.5 - 2 ms^{-1}) in wind velocity (Fig. 5a). Six storm events of different characteristics (in terms of wind and hydrodynamic conditions) for which flood/overwash events have been recorded by the video monitoring system, were isolated for detailed assessment by checking the raw, unfiltered data (S1, …, S6 in Fig. 5b-g, see also Table 4). More specifically, S1 and S2 occurred during periods of increased wind velocity (greater than 4 Beaufort) blowing from directions within the effective fetch of Poetto (effective wind events), whereas the remaining storm events (S2 till S6) occurred during periods for which no effective wind events were detected. By examining the raw wind records of the meteorological station against ECMWF forecasts during the six isolated storm events, there are cases of notable differences. During S1 the majority of the forecasted wind is found to have higher values (of about 1 - 3 ms^{-1}) compared to the records of the meteorological station (Fig. 5b). At the beginning of storm event S2, *in-situ* records are found to align well with the forecasted wind, however, after 13/04/2022 at 18.00 and onwards, the forecasted wind is found to be similarly overestimated (by 1 - 3 ms^{-1}), even if the declining trend of the forecasted wind velocity aligns with the meteorological records (Fig. 5c). The latter is also the case for the rest of the examined storm events (S3 - S6), however there are cases where the ECMWF forecasts are slightly lower (by 1.0 - 3.5 ms^{-1}) compared to the recorded wind (e.g. during S3 on 23/10/2022 between 06.00 -18.00 and during S5 on 09/03/2024 between 12.00 - 06.00).

https://doi.org/10.5194/egusphere-2025-2292
Preprint. Discussion started: 17 June 2025

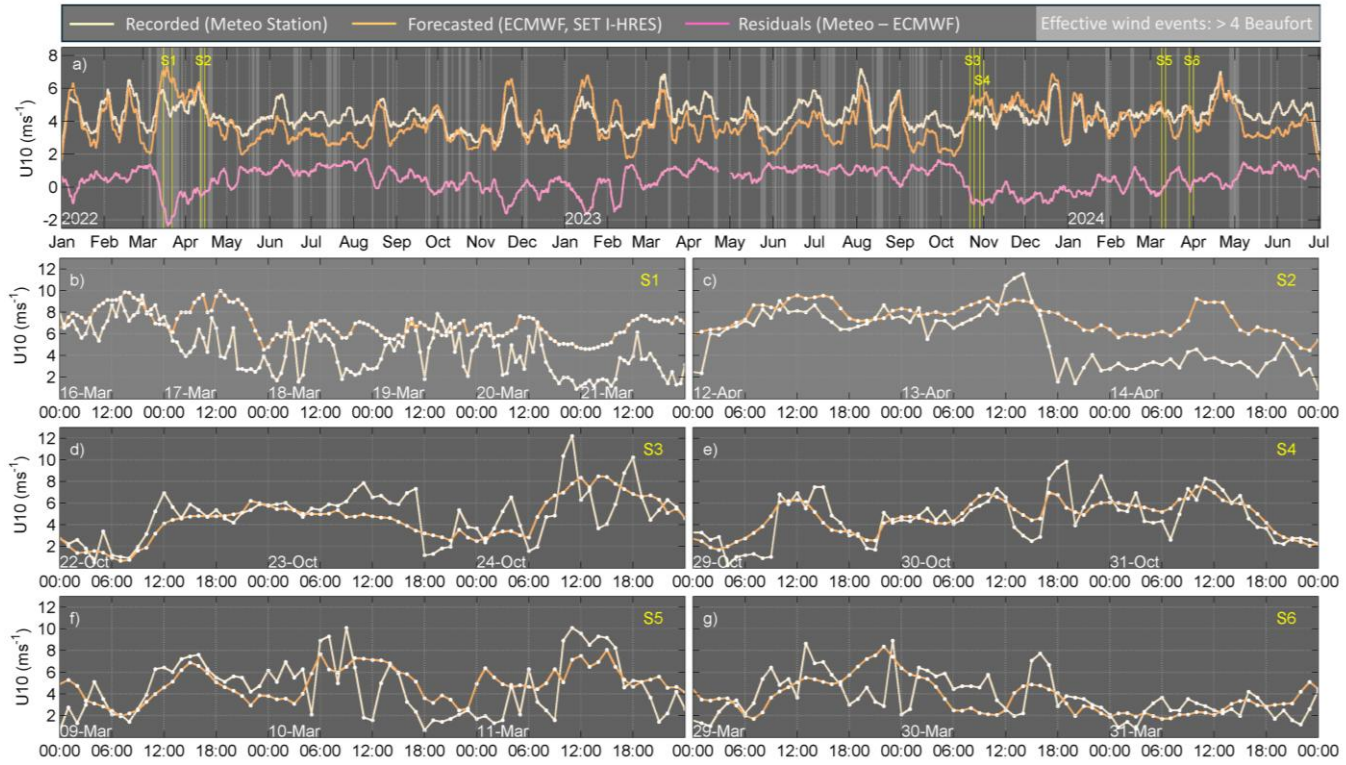

Figure 5: a) Wind velocity at 10 m height (U_{10}) of both recorded and forecasted timeseries after smoothing (window size equal to 200) during the period of 01/2022 - 07/2024. Light grey lines denote periods of detected storms/effective wind events according to the criterion of Sanchez-Arcilla et al. (2008); b) - f) Raw recorded and forecasted U_{10} timeseries of the six selected flood/overwash events used for further assessment (see Table 4 for the events' details).

The statistical evaluation provided further insights. The scatter plot of recorded and ECMWF forecasted values shows a general agreement, with the points being concentrated along the line of perfect matching (Fig. 6a). This aligns with the positive Mean Residual (Bias) estimated at 0.46 ms^{-1}, suggesting a slight systematic underestimation of the forecasted wind velocity. While this bias is relatively small, the spread of the points suggests variability in accuracy. Many points fall outside the range of the 20% error bounds, indicating instances of significant under- and over-estimations. At lower wind velocities ($U_{10} < 5$ ms^{-1}) the spread is relatively small, suggesting better accuracy for low wind velocity values; however, at higher wind velocities ($U_{10} >$ ms^{-1}) there is an increased spread and fewer points, possibly indicating greater difficulty in forecasting extreme values. The correlation coefficient (R = 0.645) indicates a strong positive linear relationship between forecasted and recorded wind velocities (p value < 0.05). On average, forecasted values deviate from the recorded values by approximately MAE = 1.57 ms^{-1}. The Scaled Mean Absolute Error (SMAE = 36.4%) suggests that the forecasted errors constitute a significant proportion of the average wind velocity, which is also visible in the scatter plot.

https://doi.org/10.5194/egusphere-2025-2292
Preprint. Discussion started: 17 June 2025

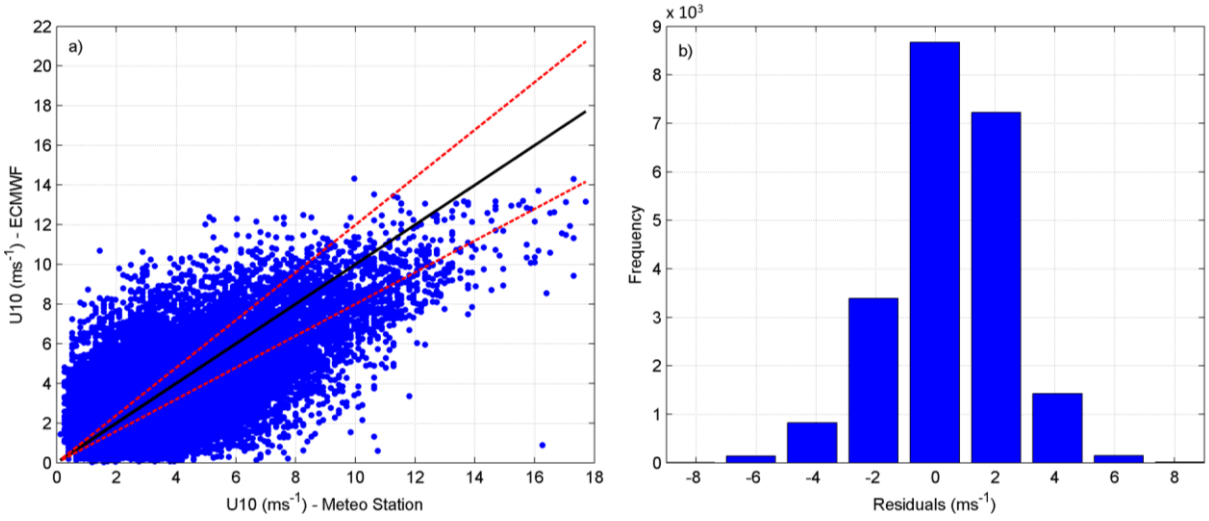

Figure 6: a) Scatterplot of wind velocities at 10 m height (U_{10}) recorded from the meteorological station versus those forecasted by ECMWF for the examined 2.5 years period; red lines: 20% error bounds, black line: perfect matching; b) Distribution of forecast errors (residuals) amongst the 21,870 total values of the timeseries.

The distribution shows that most of them residuals are close to zero (peak between ±1 ms^{-1}), indicating that the majority of forecast errors are small (Fig. 6b). Furthermore, there are more positive residuals than negative ones, at low values (between ±2 ms^{-1}) reflecting the slightly systematic underestimation of the forecasts (positive bias). Bars near the edges (e.g., at ±4 ms^{-1}) suggest some extreme forecast errors, which contribute to the relatively higher estimated RMSE (1.99 ms^{-1}) compared to MAE (1.57 ms^{-1}). SMAE (36.4%) shows that these errors are substantial relative to the recorded wind velocities. Such extreme forecast errors were not observed in the selected overwash cases.

3.2.2 Wave climate

During the 45-day validation period (16/10/2020 - 30/11/2020), the CMEMS Med-WAV re-analysis data generally follow the trends observed through the AWAC measurements. More specifically, spectral moment wave height is found to be slightly overestimated by CMEMS data (by about 0.2 m) during specific periods (e.g. on 20/10, 27/10, 16/11 and 20/22 – Fig. 7a). Notable discrepancies in peak wave period (up to 10 s) are observed during low-energy events (i.e. at times when wave heights are smaller than 0.5 m), such as on 18/10, 02/11, 20-21/11 (Fig. 7b). Mean wave direction is also found to differ significantly (by up to 130°) at periods of low wave energy (between 24/10 - 02/11 and 16/11 - 21/11), where the reanalysis data exhibit abrupt directional changes that are not observed in the AWAC records. However, at periods of increased wave heights (more than 0.5 m), CMEMS data are found to align reasonably well, having differences of about 20-25° (Fig. 7c). The overall agreement indicates that the reanalysis is reliable for capturing wave height trends, especially at periods of increased wave heights.

https://doi.org/10.5194/egusphere-2025-2292
Preprint. Discussion started: 17 June 2025

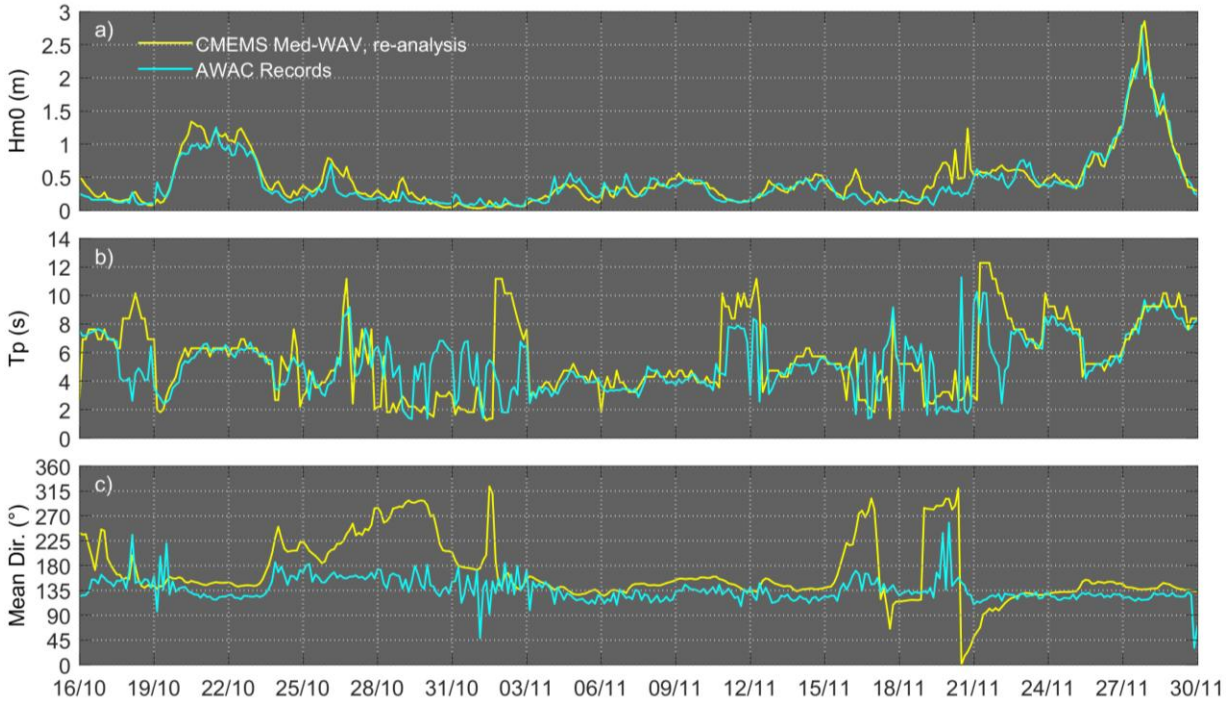

Figure 7: a) Spectral moment wave height (Hm0); b) Peak wave period (Tp); and c) Mean wave direction derived from the AWAC records and the CMEMS Med-WAV re-analysis product for a 45-day period (16/10/2020 - 30/11/2020).

Hm0 data points are generally aligned along the 1:1 reference line of perfect matching, indicating good agreement between CMEMS and AWAC data, followed by a strong correlation coefficient (R = 0.83, Fig. 8). However, a spread is noticed, particularly at Hm0 values lower than 0.5 m (Fig. 8a). MAE is 0.18 m, reflecting the average magnitude of discrepancies between AWAC and CMEMS records. SMAE has a value of 43.9%, suggesting relatively large error when scaled by the observed mean, whereas RMSE is 0.25 m, quantifying the typical magnitude of errors with a higher emphasis on larger deviations. When checking the residuals (AWAC - CMEMS), these are approximately normally distributed and centered around -0.2 m, confirming the negative bias of - 0.12 m observed in the statistical results. The majority of residuals fall within the range of ±0.2 m, indicating that most errors are moderate (Fig. 8b).

Regarding peak wave period, the scatter plot shows that points have significant deviations from the 1:1 line of perfect matching, which is also reflected by the relatively low correlation coefficient (R = 0.33). MAE is 1.7 s, whereas SMAE is 28.0%, suggesting a moderate relative error when scaled by the observed mean and RMSE is 2.5 s. The residuals distribution shows that most differences are slight, being concentrated between ± 2 s (Fig. 8d), which also reflects the positive bias of 0.26 s found in the statistical analysis. Nevertheless, the histogram reveals significant spread, with residuals ranging from -8 to 10 s, highlighting substantial errors for some predictions, particularly for low wave heights (Fig. 7a).

https://doi.org/10.5194/egusphere-2025-2292
Preprint. Discussion started: 17 June 2025

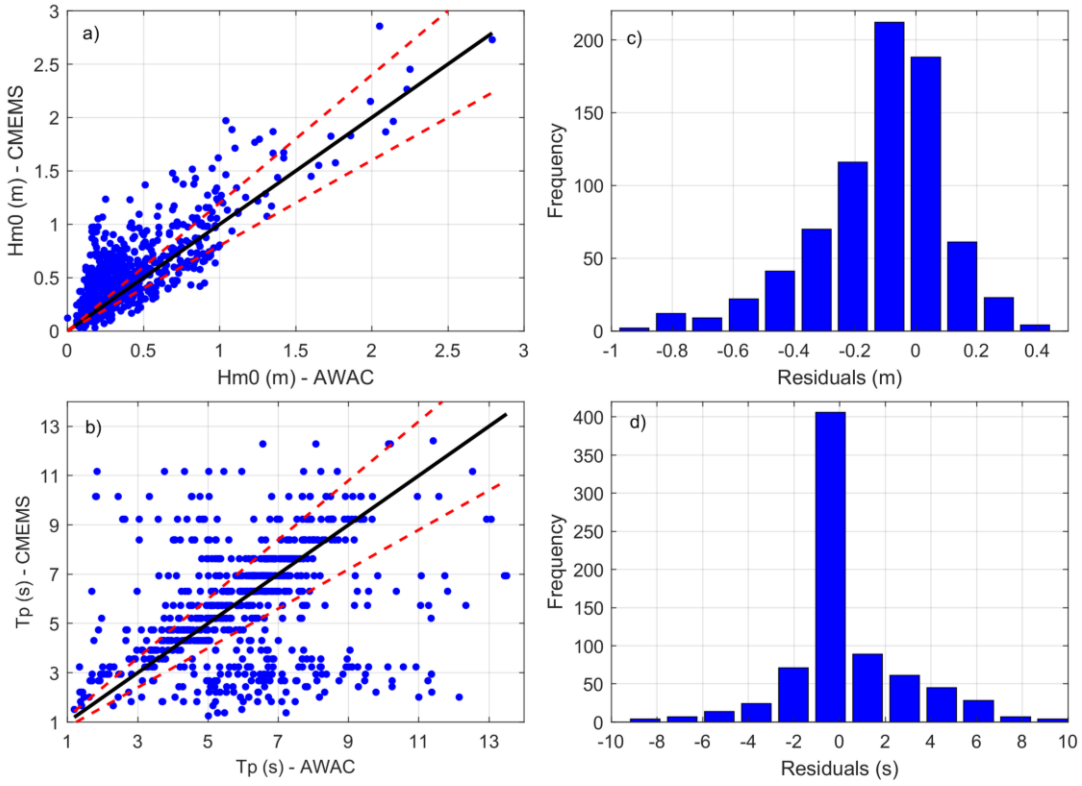

Figure 8: a) Scatter plot of spectral moment wave height (Hm0); and b) peak wave period (Tp) recorded from the AWAC versus CMEMS re-analysis for the examined 45-day period; red lines: 20% error bounds, black line: perfect matching; c) and d) Error distribution (residuals) amongst the 361 total values of the Hm0 and Tp timeseries, respectively.

Spectral moment wave heights forecasted by CMEMS Med-WAV during the examined 2.5-year period (01/01/2022 - 01/07/2024) are found to derive from directions within the effective fetch of the beach. From these values, 30% are characterized as small waves (smaller than 0.5 m), whereas 13% are found to have values more than 0.7 m and 6% more than 1 m. The most energetic events (i.e. Hm0 greater than 1 m) occur during the October - March period (Fig. 9a). The contribution of primary swell (Hm0_SW1) follows similar trends to Hm0 while secondary swell (Hm0_SW2) is found to be always smaller than 0.3 m. Wind generated waves (Hm0_WW) are found to be smaller than 0.5 m during low and moderate events (i.e. Hm0 smaller than 1 m) and of about 0.5 - 0.7 m at times when Hm0 is close to 1 m. Regarding wave periods, peak wave period (Tp), primary (Tm01_SW1) and secondary (Tm01_SW2) swell related periods range between 2.8 - 8.5 s, with higher periods at times of increased wave heights. Periods related to wind generated waves range between 1 - 2.5 s.

https://doi.org/10.5194/egusphere-2025-2292
Preprint. Discussion started: 17 June 2025

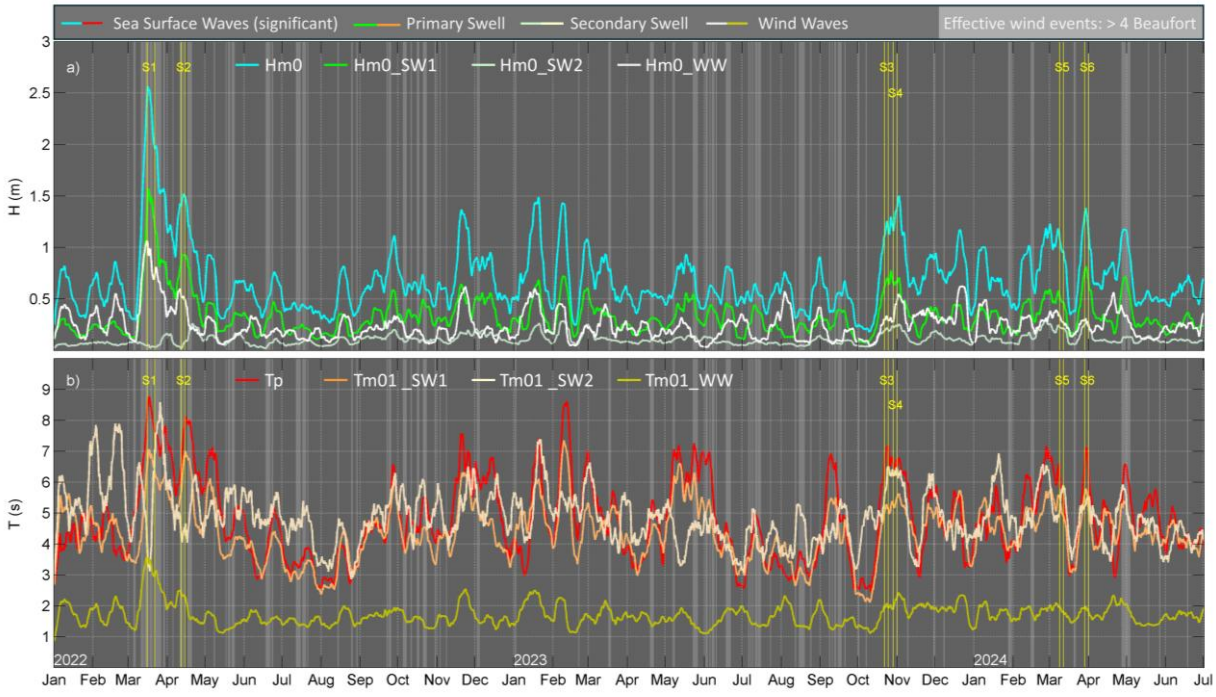

Figure 9: Smoothed (window length equal to 200) timeseries of the wave characteristics extracted from CMEMS, Med-WAV virtual buoy offshore Poetto beach. a) Spectral significant wave height (Hm0), spectral significant wind wave height (Hm0_WW), Spectral significant primary (Hm0_SW1) and secondary (Hm0_SW2) swell wave height; b) peak wave period (Tp), spectral moments (0,1) wind wave period (Tm01_WW), spectral moments (0,1) primary (Tm01_SW1) and secondary (Tm01_SW2) swell wave period.

The wave components during the selected overwash/flood events are presented in Figures 10 and 11. Event S1 was found to have the highest magnitude and duration during the examined 2.5 years period with forecasted spectral wave height (Hm0) values greater than 1.5 m and corresponding peak periods (Tp) ranging between 8 - 11 s, for a period of 4.5 days (16-21/03/2022) (Fig. 10a and 11a). During this event, wind generated waves heights (Hm0_WW) were between 0.5 - 1.2 m, with a peak at about 2.0 m on 16/03/2022, and corresponding periods (Tm01_WW) were between 2.9 - 4.8 s. Primary swell wave heights (Hm0_SW1) were generally 0.1 to 0.2 m lower than Hm0 in most cases, with the exception of the Hm0_WW peak on 16/03/2022. During event S2, Hm0 is found to range between 1.3 - 2.0 m with corresponding peak periods of about 6.4 - 9.0 s. Primary swell is found to be the main wave component. Secondary swell wave heights are found to be of zero value for both S1 and S2 events. Events S3, S4, S5 and S6 have a duration of 3 days and are found to follow similar patterns. During the first day of these events, forecasted waves are lower than 1 m, while waves are found to progressively grow in height, reaching their peak values of about 1.6 m (S3), 1.8 m (S4, S5) and 2.2 m (S6).

https://doi.org/10.5194/egusphere-2025-2292
Preprint. Discussion started: 17 June 2025

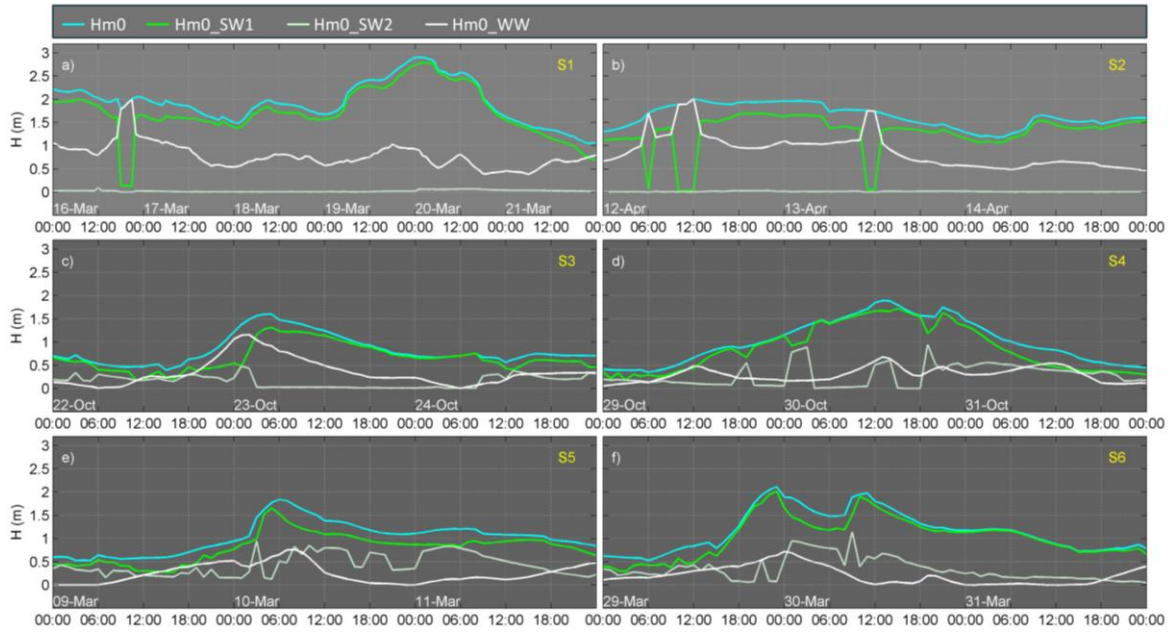

Figure 10. Wave heights extracted from CMEMS, Med-WAV virtual buoy offshore Poetto beach during the six isolated flood/overwash events recorded from the optical system (see Table 4 for the events' details).

420

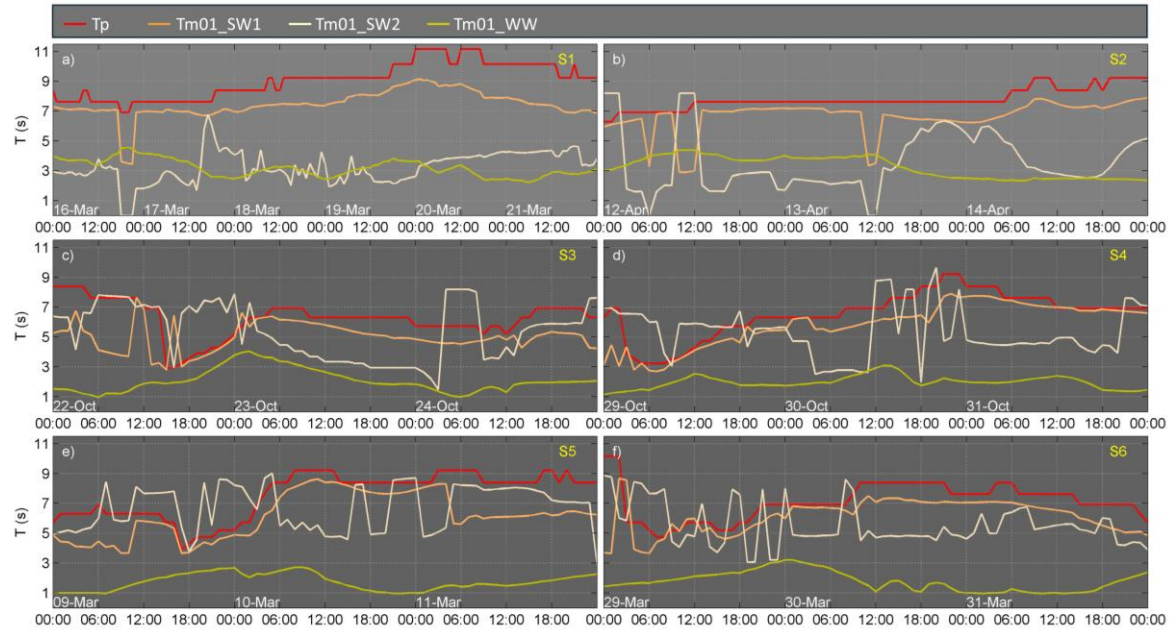

Figure 11. Wave periods extracted from CMEMS, Med-WAV virtual buoy offshore Poetto beach during the six isolated flood/overwash events recorded from the optical system (see Table 4 for the events' details).

https://doi.org/10.5194/egusphere-2025-2292
Preprint. Discussion started: 17 June 2025

3.2.3 Sea Level

The forecasted sea level timeseries are found to align well with the sea level recorded from the tide gauge, located 2.1 km away from the CMEMS V-PHY point (see Fig. 1b). For the examined 2.5 years period, recorded sea level is found to be slightly higher than forecasted sea level for most of the examined period (Fig. 12a).

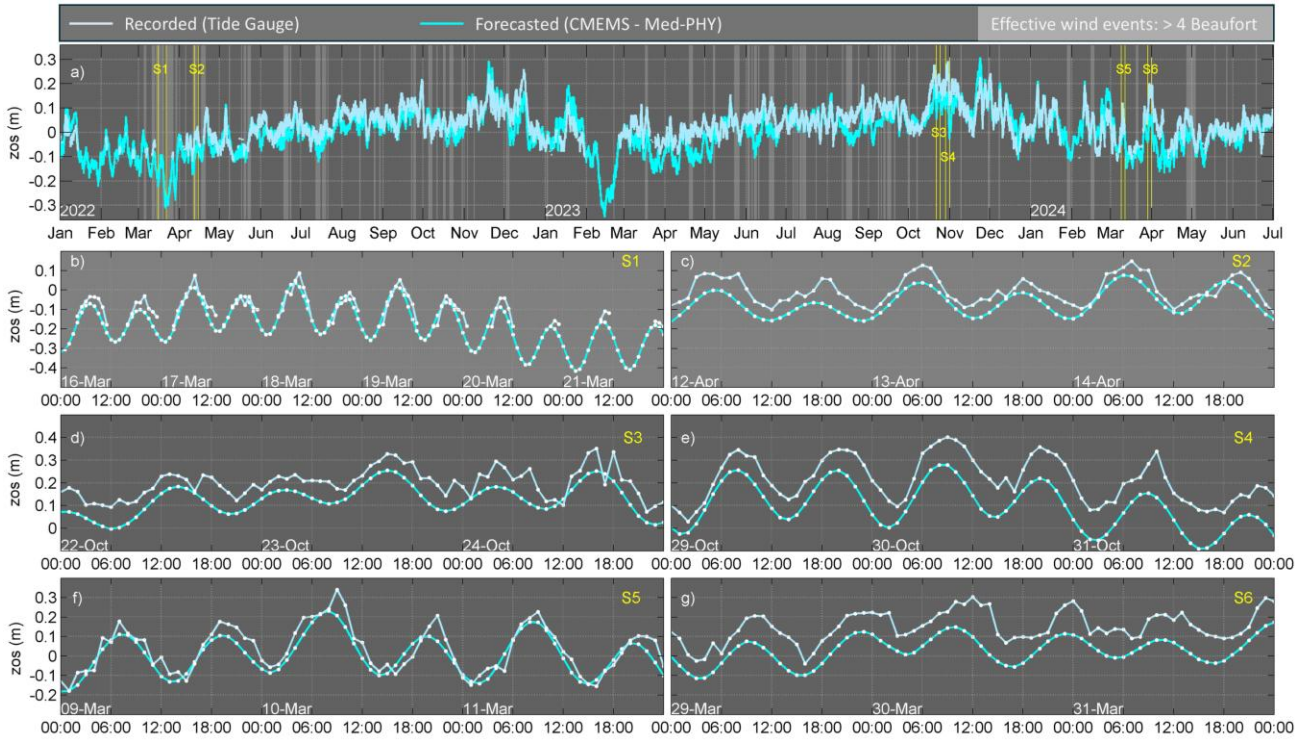

Figure 12. a) Sea level recorded from the logger and forecasted from CMEMS Med-PHY after smoothing (window size equal to 20) during the period of 01/2022 – 07/2024. Light grey lines denote periods of detected storms/effective wind events according to the criterion of Sanchez-Arcilla et al. (2008); b) - f) Raw recorded and forecasted sea level timeseries of the six selected overwash/flood events used for further assessment (see Table 4 for the events' details).

During the six monitored overwash/flood events, recorded sea level is found to be slightly higher with maximum differences of about 0.1 m (Fig. 12b-d). Events S1 and S5 are found to fit almost perfectly with the recorded values, whereas sea level forecasts during events S2, S3, S4 and S6 are found to have lower values, compared to the tide gauge records (of about 0.1 m). Overall, the forecasted sea level values used by NEPTUNE-EWS are found to be slightly underestimated, but in a minor way that has limited effect on the early warning system.

When examining the statistical results, the correlation coefficient was found to have a value of R = 0.85, indicating that the forecast is fairly reliable and that the two datasets generally follow a similar trend. The latter is also evident when checking the scatter plot, where points are dense within the range of the 20% error bounds (Fig. 13a). On average, forecasted sea levels were found to deviate from the recorded values by MAE = 0.047 m and by RMSE = 0.059 m, which tends to emphasize larger

https://doi.org/10.5194/egusphere-2025-2292
Preprint. Discussion started: 17 June 2025

445 errors more than smaller ones. The mean Residual (Bias) was estimated at 0.014 m, suggesting that on average, the CMEMS forecasted data are systematically slightly underestimating the recorded sea level. This is also consistent with the distribution of the residuals, where most values are being concentrated at low errors (mostly positive) following an almost normalized distribution (Fig. 13b).

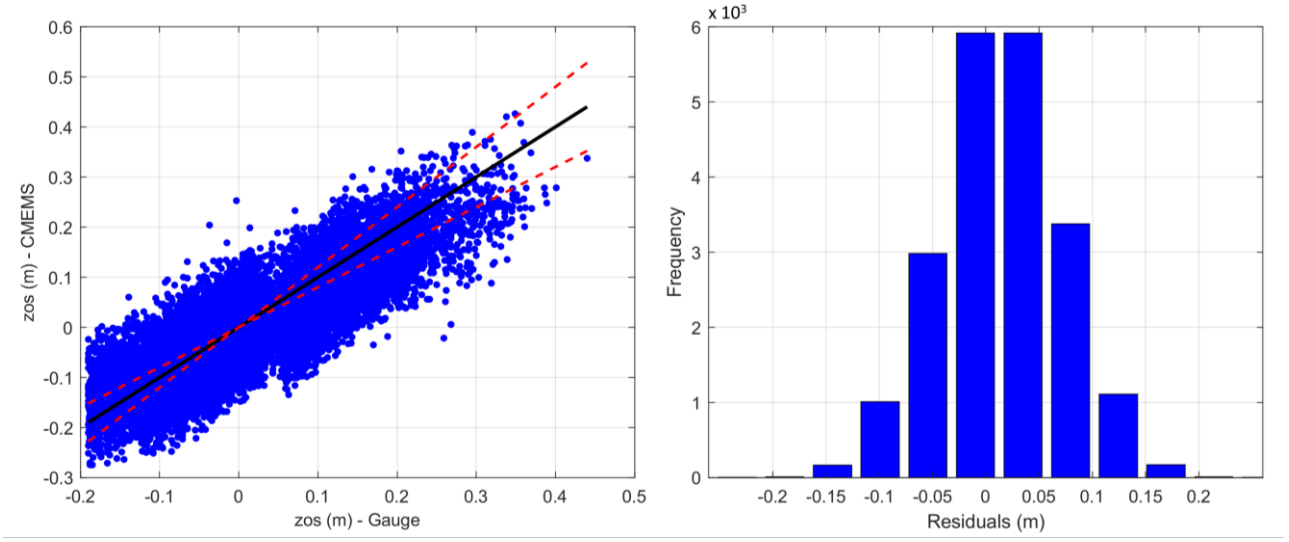

450 **Figure 13. a) Scatter plot of sea surface height (zos) recorded from the tide gauge versus the forecasted by CMEMS for the examined 2.5 years period; red lines: 20% error bounds, black line: perfect matching; b) Distribution of forecast errors (residuals) amongst the 21,870 total values of the timeseries.**

455 SMAE was found to be 188.9%, suggesting that for some records (especially for values close to zero), the forecast might be off by a large percentage, although the magnitude of sea level variation is small compared to other contributions. It has to be noted that the tide gauge is located inside Cagliari's port, distanced 2.6 km away from the CMEMS Med-PHY virtual buoy (see Fig. 1b).

3.3 Assessment of NEPTUNE-EWS's Performance

460 The daily forecasted characteristics of the six flood/overwash events monitored by the coastal videocameras, are reported in Table 4. Event S1 is the event with the highest magnitude and duration with maximum wave height of 2.9 m, nominal wave direction from the SE, maximum wind speed of 9.6 ms^{-1}, nominal wind direction from the SE and a duration of 6 days. During the 3-day event S2, wind was blowing from the SE for the first two days having an intensity of more than 5 Beaufort, whereas at the last day wind is found to be significantly lower with nominal direction from the E. At the same time, mean significant
465 daily wave heights were about 1.4 - 1.8 m, deriving from the SE, with corresponding mean peak periods of about 7.2 - 8.5 s for the whole period of the event. Events S1 and S2 follow the criteria of Sanchez-Arcilla et al. (2008), and thus, are considered as effective wind events greater than 4 Beaufort. This is not the case for events S3 - S6 who are found to be of lower magnitude

https://doi.org/10.5194/egusphere-2025-2292
Preprint. Discussion started: 17 June 2025

or/and have wind direction blowing from directions outside the effective fetch of Poetto. Nevertheless, overwash and flooding have been recorded from the video monitoring system during these events.

Table 4. Forecasted wind and wave characteristics of the six monitored overwash/flood events.

ID	Date	Mean U10 (ms^{-1})	Max U10 (ms^{-1})	Wind Dir. (°)	Mean Hs (m)	Mean Tp (s)	Max Hs (m)	Max Tp (s)	Wave Dir. (°)
S1	16/03/2022	7.4	9.6	121	2.1	7.6	2.2	8.4	139
	17/03/2022	4.6	7.6	106	1.8	7.8	2.0	8.4	137
	18/03/2022	3.8	7.1	120	1.8	8.8	2.0	9.2	136
	19/03/2022	5.0	7.9	126	2.3	9.4	2.9	10.1	137
	20/03/2022	3.4	7.1	122	2.4	10.8	2.9	11.1	136
	21/03/2022	2.5	6.1	80	1.3	9.8	1.6	10.1	127
S2	12/04/2022	6.9	9.0	121	1.8	7.2	2.0	7.6	136
	13/04/2022	6.6	11.5	123	1.7	7.6	2.0	7.6	137
	14/04/2022	3.3	5.1	81	1.4	8.5	1.7	9.2	131
S3	22/10/2023	3.8	7.0	225	0.6	6.3	1.0	8.4	187
	23/10/2023	5.3	7.9	223	1.2	6.3	1.6	6.9	135
	24/10/2023	5.6	12.1	277	0.7	6.1	0.8	6.9	174
S4	29/10/2023	3.6	7.5	100	0.6	4.9	1.0	6.9	165
	30/10/2023	5.6	9.8	116	1.6	7.3	1.9	9.2	139
	31/10/2023	5.0	8.3	322	0.8	7.4	1.5	8.4	180
S5	09/03/2024	4.4	7.6	312	0.6	5.8	0.9	6.9	172
	10/03/2024	4.5	10.1	301	1.4	8.1	1.8	9.2	145
	11/03/2024	4.9	10.1	292	1.0	8.7	1.2	9.2	193
S6	29/03/2024	4.3	8.9	151	1.0	6.2	2.1	10.1	154
	30/03/2024	4.3	7.7	141	1.6	7.7	2.0	8.4	136
	31/03/2024	2.4	4.2	154	1.0	7.4	1.2	8.4	132

NEPTUNE-EWS, is set to estimate TWL by using the six aforementioned empirical methods for wave run-up estimations. The performance of each method during the monitored event of the longest duration and magnitude (event S1) for the cross-shore locations P1 and P2 is shown in Fig. 14c-d. Beach conditions during the events were examined through the records of the coastal videocameras. An example of overwash, flood and no trace detection is shown in Fig. 14a-b for event S1 at locations P1 and P2 (see Annex for further investigation of the camera records). During event S1, the formulae of Nielsen and Hanslow (1991) and Ruggiero et al. (2004) are found to significantly underestimate wave run-up contribution to TWL for both P1 and P2 locations. The approximations of Hunt (1959), Holman (1986) and Douglas (1992) are also found to underestimate flooding (during 19-21/03/2022, see Fig. 14c-d). Overall, in the case of Poetto the formula of Stockdon et al. (2006) is found to be the only to provide realistic results, and thus wave run-up estimates are based on this approach (Fig. 15 and 16).

https://doi.org/10.5194/egusphere-2025-2292
Preprint. Discussion started: 17 June 2025

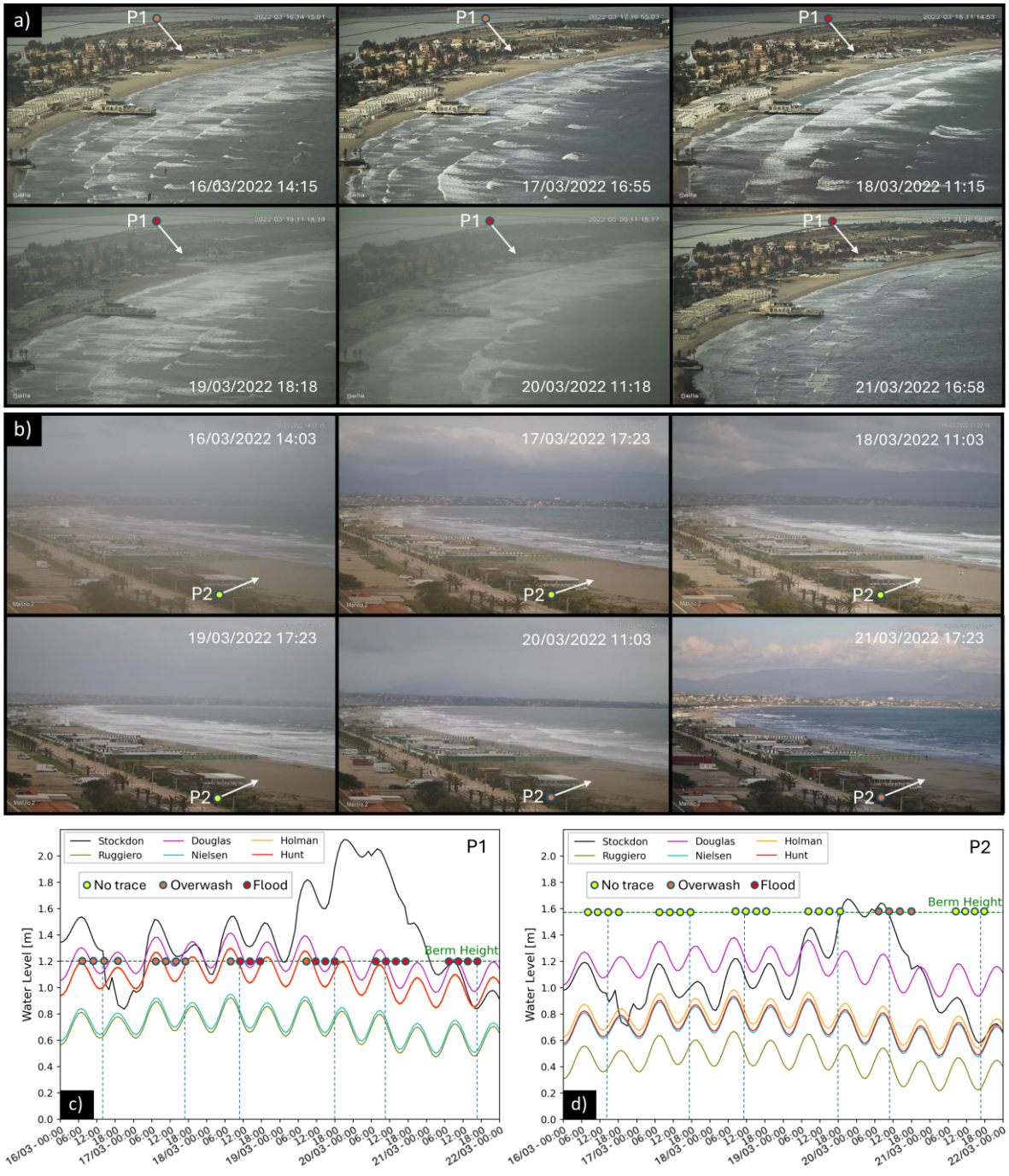

Figure 14. a) and b) Selected daily images during event S1 recorded from coastal videocameras CAM1 and CAM2 at locations P1 and P2, respectively. c) and d) Projected Total Water Level (TWL) after the use of six typical empirical equations for wave run-up estimation during event S1 at locations P1 and P2, respectively; points show the monitoring periods of the videocameras and the flood state (optical observations); vertical dashed lines delimit the time during which images shown in a) and b) were retrieved.

https://doi.org/10.5194/egusphere-2025-2292
Preprint. Discussion started: 17 June 2025

Energetic wave conditions (forecasted Hm0 greater than 2 m) were observed during the first day of event S1, followed by a decrease on the second day (17/03/2022). Waves increased over the next two days, reaching a peak of forecasted maximum Hs of 2.9 m during 19-20/03/2022. At midday of 20/03/2022 and onwards, a significant reduction in wave heights is observed (Fig. 10). The projected TWL for locations P1 and P2 is shown in Fig. 15a-b. At both locations, a similar trend is observed with increasing TWL at periods of energetic wave conditions, having however different magnitude.

There are several periods where the projected TWL is found to exceed the morphological threshold (i.e. berm height of this location, recorded at the closest available date to event S1). These periods are found to be consistent with times of recorded overwash/flood evidence observed through the video records. More specifically, overwash evidence have been observed for P1 location, starting from the beginning of the event (16/03/2022) until midday of 18/03/2022. During this period, NEPTUNE's TWL predictions exceeded the 1.2 m morphological threshold up to 0.3 m for most of the time, with the exception of certain periods (from 18/03/2022 17:00 until 17/03/2022 06.00 and from 18/03/2022 01:00 until 07:00). The first flooding trace is observed from 18/03/2022 11:00 onwards, till the end of the event. During this time, the projected TWL is found to range between 1.2 and 2.1 m, exceeding the berm height threshold for 68 hours (from 18/03/2022 05:00 until 21/03/2022 01:00). Regarding location P2, threshold exceedance (by 0.1 m) occurred for a limited time (for 6 hours) between 19 - 20/03/2022. The latter aligns well with the recorded overwash observed from the optical data on 20/03/2022, while for the remaining days of the event no evidence of overwash has been recorded. Overall, NEPTUNE-EWS's predictions are found to align well with the optical records for this event.

At the beginning of event S2, and for half of its duration (from 12/04/2022 02.00 until 13/04/2022 16.00), the recorded wind is found to have magnitude of more than 6.0 ms^{-1} and reduced to less than 4.0 ms^{-1} for most of the remaining period (Fig. 5b). Maximum recorded U_{10} values are found to range between 5 – 6 Beaufort (8.0 – 11.9 ms^{-1}) occurring for 5 hours between 13/04/2022 11.00 - 16.00. For this event, forecasted Hm0 is found to range between 1.2 - 2.0 m for the whole 3-day period of the event with the only decreasing trend observed between for one day (from 13/04/2022 05.00 - 14/04/2022 05.00 (Fig. 10b). These observations align well with the TWL forecasted by NEPTUNE-EWS for locations P1 and P2 that suggest a general decreasing trend in TWL from 13/04/2022 08.00 - 14/04/2022 02.00, with the exception of three hours (on 13/04/2022 between 13.00 - 15.00) (Fig. 15c-d). The latter could be attributed to storm surge event generated by barometric differences and increased wind velocities, which were recorded during this time (see Fig. 5b). At location P2, TWL predictions never exceed the morphological threshold, suggesting that no overwash/flooding occurred during event S2. This aligns well with the optical records as there was no trace of ovewash/flooding for this period (Fig. 15d). On the other hand, there are five different periods during which NEPTUNE-EWS projected TWL exceeded the 1.2 m threshold for location P1: i) for three hours between 12/04/2022 15.00 - 18.00; ii) for one hour on 13/04/2022 00.00 - 01.00; iii) for seven hours between 13/04/2022 02.00 - 09.00; iv) for four hours between 13/04/2022 15.00 - 19.00; and v) for at least six hours between 14/04/2022 06.00 - 00.00 (last projected hour). When checking the available optical records for this event, there is no overwash/flooding trace observed during the three-hour exceedance period. However, overwash traces are observed exactly after the seven-hour TWL

https://doi.org/10.5194/egusphere-2025-2292
Preprint. Discussion started: 17 June 2025

525 exceedance on 13/04/2022, as well as during the four-hour TWL exceedance on the same day. In addition, evidence of overwash has been recorded during the last day of event S2 at 14/04/2022 08.00, followed by a flood trace at 11:00 and two overwash traces at 14:00 and 17:00, suggesting a decrease in TWL which is confirmed by NEPTUNE-EWS's predictions for this period (Fig. 15c).

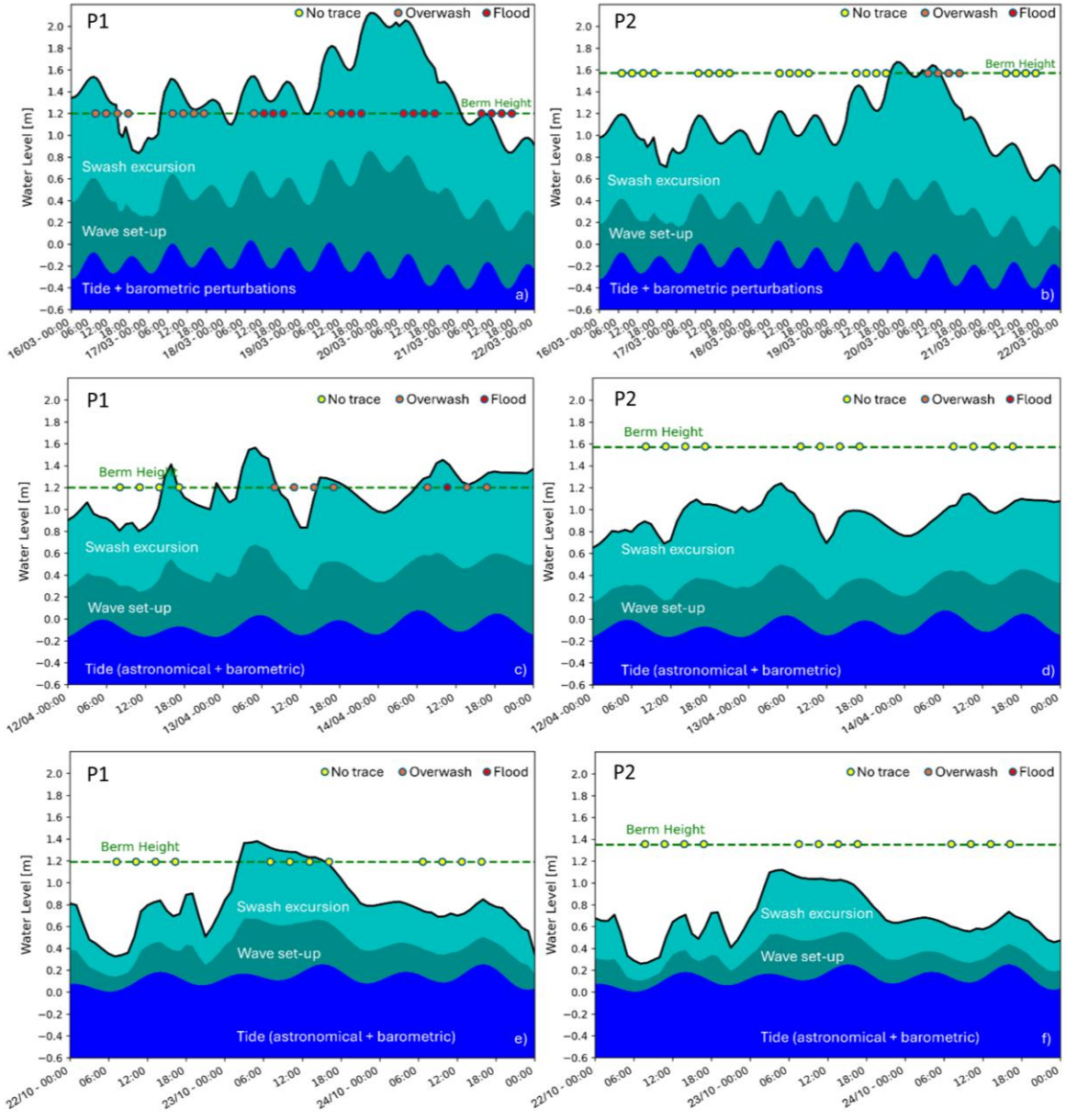

530 **Figure 15. Projected TWL and its components, as well as overwash, flood and no trace records deriving from the video monitoring system for event a)-b) S1; c)-d) S2; and e)-f) S3, at locations P1 and P2.**

https://doi.org/10.5194/egusphere-2025-2292
Preprint. Discussion started: 17 June 2025

Wave action is found to be mild (projected Hm0 below 1.0 m) for most of the three-day duration of event S3, with the exception of seven hours (between 22/10/2023 11:00 - 23/10/2023 18:00) when projected Hm0 is found to have values between 1.0 - 1.6 m (Fig. 10c). This is also the time when projected TWL by NEPTUNE-EWS reaches its peak, following a similar increasing and declining trend (Fig. 15e-f). For location P2, there is no exceedance of the morphological threshold, which is validated by the optical records as no overwash/flood trace has been observed for the whole period (Fig. 15f). Regarding location P1, NEPTUNE-EWS forecasted a TWL exceeding the 1.2 m morphological threshold for 15 hours (between 23/10/2023 02:00 - 17:00, Fig. 15e). However, there was no overwash/flood trace recorded by the coastal videocamera during this period. The latter could be attributed to the limited exceedance of the morphological threshold by 0.2 m for two hours, 0.1 m for six hours and by less than 0.1 m for the remaining time.

During event S4, waves offshore Poetto beach are found to have mild heights at the beginning of the event (29/10/2023 00:00 - 09:00) with projected Hm0 heights of about 0.5 m. Afterwards, Hm0 is found to progressively increase (almost linearly) reaching its peak at 1.8 m on 30/10/2023 13:00, slightly declining to a value of 1.5 m till 30/10/2023 21:00 and then follow a declining trend till a value of 0.6 m for the remaining period (Fig. 10d). This trend is consistent with the projected TWL for both locations (Fig. 16). Regarding location P1, the recorded traces align well with the overwash/flooding threshold. No trace is observed from the optical information retrieved on 29/10/2023, whereas an overwash trace is observed close to the starting date of threshold exceedance on 30/10/2023 07:00, followed by flood traces until 30/10/2023 17:00 (Fig. 16a). Flood traces are recorded for the next day during the available optical records (between 31/10/2023 07:00 - 17:00), which most possibly are the outcome of flood intensity of the previous day. Regarding location P2, NEPTUNE-EWS failed to project coastal flooding that was recorded from the optical system on 30/10/2024 and onwards (Fig. 16b). During this period, TWL was below the morphological threshold set at 1.35 m, with a slight exceedance projected for 3 hours at the end of 30/10/2024. However, the morphological thresholds set for this event are based on the topographic records retrieved on 09/06/2024.

Event S5 follows a similar pattern with event S3, having however different magnitude. At the beginning of the event the approaching waves are forecasted to have Hm0 of about 0.6 m, until 09/03/2024 17:00 (Fig. 10e). From this time onwards waves are found to increase in height, reaching a peak Hm0 value of 1.6 on until 10/03/2024 06:00 and then progressively decrease until 11/03/2024 00:00 when Hm0 value is found to have a value of about 1.1 m. After this hour, Hm0 values slightly increase to reach a value of about 1.3 m on 11/03/2024 08:00 and then progressively decrease to a value of 0.9 m at the end of the event. This trend is consistent with the TWL projected by NEPTUNE-EWS (Fig. 16c-d). There was no overash/flood trace recorded by the optical system for both P1 and P2 locations, from the available records retrieved on 09/03/2024. On the contrary, overwash trace is recorded for P1 location followed by flood traces on 10/03/2024, which is consistent with the projected TWL that exceeded the 1.05 m threshold during this day up to 0.8 m at 06:00 (Fig. 16c). On 11/03/2024 TWL exceeded the morphological threshold up to 0.3 m for a period of 12 hours (from 00:00 until 12:00), while for the same day overwash traces are recorded from the coastal videocamera for this location. Regarding location P2, overwash traces are observed from the available records on 10 and 11/03/2024 (Fig. 16d). The latter is consistent with the projected TWL that exceeded the 1.1 m berm heigh for this location up to 0.3 m for a duration of 8 hours on 10/03/2024.

https://doi.org/10.5194/egusphere-2025-2292
Preprint. Discussion started: 17 June 2025

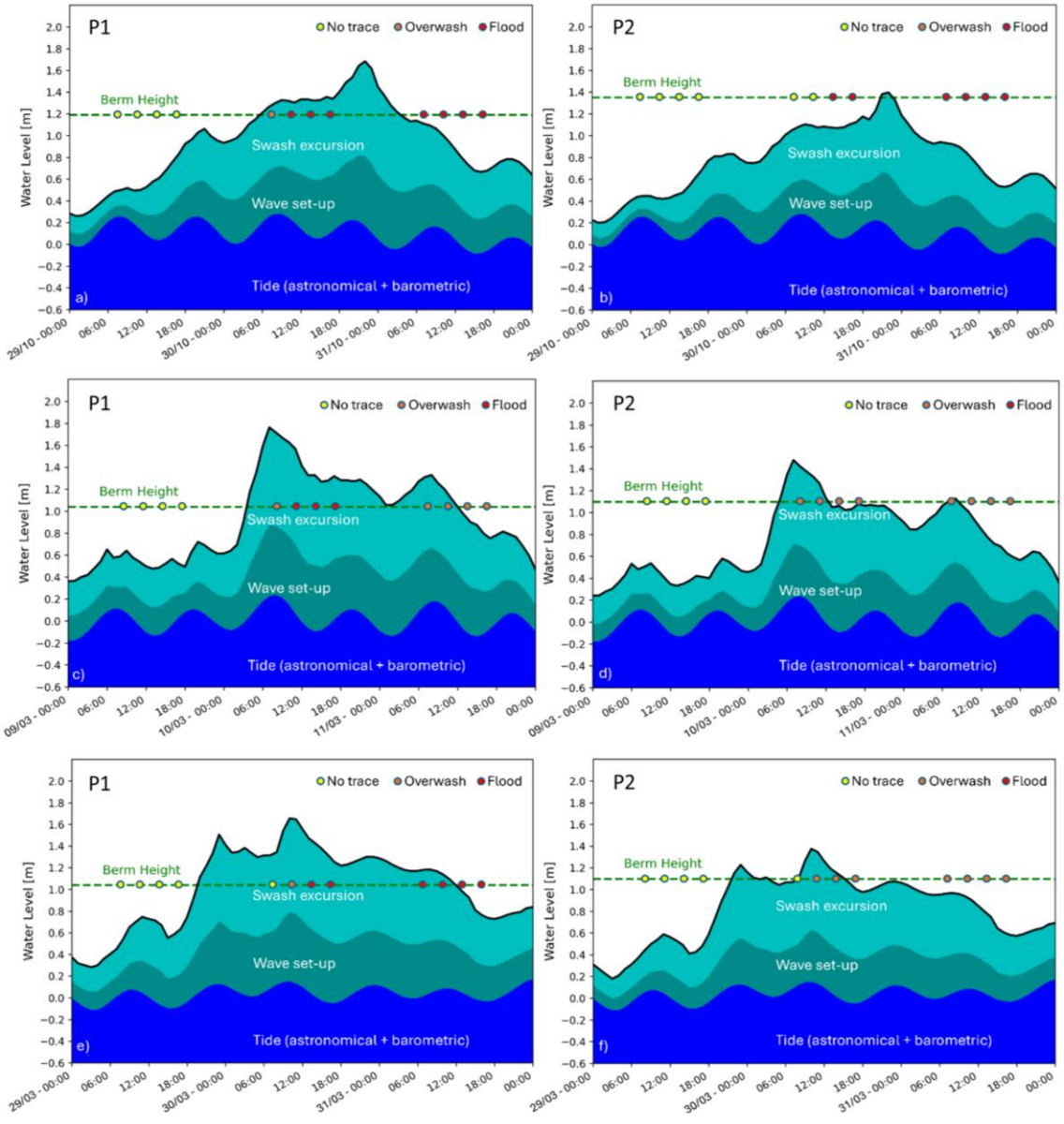

Figure 16. Projected TWL and its components, as well as overwash, flood and no trace records deriving from the video monitoring system for events a)-b) S4; c)-d) S5; and e)-f) S6 at locations P1 and P2.

During event S6, increased wave activity (Hm0 values above 1.0 m) was forecasted for 53 hours between 29/03/2024 16:00 - 31/03/2024 21:00 (Fig. 10f), which led to increased TWL for the same period (Fig. 16e-f). At location P1, TWL exceeded the 1.05 m morphological threshold for most of the period of increased wave activity (Fig. 16e). Interestingly, no overwash/flood trace was detected from the records of the coastal videocamera on 30/03/2024 07:00, 12 hours after the starting hour of

https://doi.org/10.5194/egusphere-2025-2292
Preprint. Discussion started: 17 June 2025

projected TWL above the 1.05 m threshold. However, an overwash trace is recorded at the next available record at 11:00, followed by flood traces at 14:00 and onwards till the end of the event. At location P2, threshold exceedance is reported for two periods of limited duration i) for 3 hours (21:00 - 00:00); and ii) for 6 hours (09:00 - 15:00) on 30/03/2024 (Fig. 16f). No flood trace is recorded from the optical information until 30/03/2024 11:00, when an overwash trace is detected at the time of the highest projected TWL (1.4 m). Overwash traces are recorded till the end of the event for this location, during the available times of the optical information.

Overall, the forecasts of NEPTUNE-EWS are found to align well with the six monitored overwash/flood records. Nevertheless, the following trend is observed: Flood events are validated at times when the projected TWL exceeds the morphological threshold for more than 6 hours and is more than 0.2 m above the threshold. In different cases, overwash traces or no traces were recorded by the coastal videocameras (e.g. S1 – Fig. 15a-b and S3 – Fig. 15e-f). Considering this trend, simulated events S1, S2 and S5 are found to be in good agreement with the video information. However, there are single cases when NEPTUNE failed to project the recorded state during events S4 and S6. During event S4 flooding is recorded for two consecutive days for location P2 which was not projected by the system (Fig. 16b), whereas during event S6 there was no overwash/flooding trace reported from the camera records at a time when the system projected TWL above the morphological threshold (Fig. 16e).

4. Discussion

The forecasted wind and sea level data generally aligned well with the *in-situ* records of the meteorological station and the tide gauge for the examined 2.5-year period demonstrating similar trends. The forecasted wind directions at the location of the ECMWF point are found to be consistent with the meteorological station records. However, ECMWF wind velocity forecasts were found to be generally underestimated by up to 2-3 ms^{-1} compared to the wind records, particularly for high values of wind velocity (greater than 5 ms^{-1}) blowing from the effective fetch directions of Poetto beach (Fig. 4). The recorded wind velocities are found to be lower than ECMWF's forecasts during the monitored overwash/flood events S1 and S2, which have been categorized as effective wind events (Fig. 5b-c). In contrast, during events S3 until S6, the recorded wind velocities were higher, particularly at peak wind intensities, although the general trend remained similar (Fig. 5d-g). However, it is important to consider that ECMWF forecasts are provided at a point located at a distance of 11.2 km offshore the meteorological station, which is deployed at a low elevation inside the port of Cagliari and may reflect sheltering of the headland and relief of Sella del Diavolo that delimits the bay (see Fig. 1b). Nevertheless, the latest up-to-date analytical studies that examined ECMWF U_{10} forecasts against *in-situ* records, agree that predictions tend to systematically underestimate wind velocity (U_{10}), with a similar rate (e.g. Cavaleri et al., 2024; Haiden et al., 2024). Comparison of the wave characteristics between the AWAC records and CMEMS Med-WAV re-analysis data are found to align reasonably well. Spectral moment wave heights and peak wave periods deriving from CMEMS are found to be slightly overestimated (RMSEs of 0.2 m and 2.5 s, respectively), especially at times of low energy conditions. Regarding wave direction, a difference of about 20-25° is observed at periods of increased wave heights. These findings are in agreement with the results of Ruju et al. (2019) who examined *in-situ* wave records of an

https://doi.org/10.5194/egusphere-2025-2292
Preprint. Discussion started: 17 June 2025

AWAC profiler against forecasted wave characteristics of the WaveWatch III (WWIII) model downscaled for Poetto beach. The AWAC was deployed at a similar position with the deployment of 2020 (see Fig. 1b) and at the same depth (-18 m) for a 40-day period during 2017. In this work, it was found that while WWIII correctly addressed spectral moment wave height, peak wave period was found to be overestimated, especially under energetic conditions. Moreover, WWIII model was found to underestimate the directional spread by 25°. Both WWIII and WAM 4 used by CMEMS Med-WAV re-analysis are third-generation wave models that solve the wave action density spectrum using a discrete grid in spectral and spatial domains, including the effects of nonlinear wind-wave interactions. Sea level forecasts provided from CMEMS Med-PHY, are found to be in good agreement with the tide gauge records, with slight underestimations (up to RMSE = 5.9 cm), especially during high-water periods. This consistent underestimation could also be explained by the spatial offset between the CMEMS grid point and the tide gauge location, but also aligns well with the findings of recent studies (e.g. Irazoqui Apecechea et al., 2023; Perez-Gomez et al., 2024). Despite these minor discrepancies, sea level forecasts successfully captured the evolution trends of the recorded timeseries.

Six different empirical methods used for wave run-up estimations were tested. When summed as a component to the estimation of TWL, the wave run-up estimates deriving from the formulae of Stockdon et al. (2006) were found to give the most realistic results for the case of Poetto beach. It should be noted that Hunt's (1959) approximation was primarily developed for engineered hard structures with steep slopes, whereas the formulae of Holman (1986) and Douglas (1992) were based on measurements conducted on reflective beach conditions. This explains their low accuracy in wave run-up estimates for an intermediate sloped beach like Poetto. On the other hand, the parameterizations of Nielsen and Hanslow (1991) and Ruggiero et al. (2004), developed for mildly sloped dissipative beaches, also proved inadequate in providing accurate estimates for Poetto, particularly during energetic events. The outperformance of Stockdon et al. (2006) approach is consistent with other studies that evaluated the capability of several empirical formulae to predict wave run-up excursion on sandy beaches with mild foreshore slopes under increased wave action, despite reported cases of underestimations (e.g., Vousdoukas et al., 2009; Vousdoukas et al., 2012; Senechal et al., 2011; Paprotny et al., 2014; Aniskiewicz et al., 2016; Cohn and Ruggiero, 2016; Atkinson et al., 2017; Gomez da Silva et al., 2020; Bujak et al., 2023).

Regarding the contribution of both wave set-up and swash excursion components in TWL, it is evident that the inclusion of wave provided the most realistic results (Fig. 14 to 16). This comes in contrast with the findings of previous studies, which suggests that TWL can be approximated as the sum of the mean sea level, tide and level variations associated with storm surges (Rulent et al., 2020; Caruso and Marani, 2022; Croteau et al., 2023). Furtermore, Cabrita et al. (2024) provided a detailed investigation of the different methods used for TWL estimations and concluded that the approaches which involve calculating extreme values from a combined time series or the water level time series plus the extreme value of wave setup, yield the most realistic results, excluding the wave run-up (in this case swash excursion) component. It seems that the selection of individual TWL components is a complicated task, being subjected by limitations arising from the spatial resolution used for the computation of TWL, and the different environments.

https://doi.org/10.5194/egusphere-2025-2292
Preprint. Discussion started: 17 June 2025

NEPTUNE-EWS proved to be capable of providing accurate flooding predictions at the selected cross-shore locations of Poetto beach. Flooding forecasts were found to be in good agreement with the six overwash/flooding of different characteristics monitored by the coastal videocameras, especially during periods of high wave conditions. During energetic events S1 and S2 (characterized by incoming wave heights greater than 1.5 m for most of the event's duration) the recorded overwash and flooding traces at both locations matched with the projected periods of TWL threshold exceedance. In event S3, wave action was in general mild (wave heights lower than 1 m) with the exception of 18 hours during which wave heights reached a peak of 1.6 m, leading to a limited exceedance of the TWL threshold at P1 location. However, no overwash or flooding traces were recorded, likely due to the marginal exceedance during this time (below 0.2 m for brief periods). Event S4 presented a progressive increase in wave heights, peaking at 1.8 m on 30/10/2023. Overwash and flooding traces at P1 aligned well with projected TWL exceedances. However, at P2, NEPTUNE-EWS underpredicted the flood traces recorded on 30/10/2023 and onwards. These isolated failures could be attributed to the ever-changing beach morphology that affects the morphological threshold set by the system (in this case the berm height), which was recorded at different times of the simulated events. For event S5, wave heights peaked at 1.6 m, with TWL exceeding thresholds at both locations. Overwash and flooding traces at P1 and P2 matched NEPTUNE's predictions, demonstrating robust performance. Event S6 was characterized by increased wave activity (wave heights greater than 1 m for 53 hours), leading to TWL threshold exceedances at both locations. At P1, flooding traces were recorded later than the initial exceedance, indicating potential lag effects. At P2, observed overwash aligned with projected TWL peaks.

Overall, it was found that at times when the projected TWL exceeded the morphological threshold by less than 0.2 m for a duration of less than 6 hours, overwash traces or no traces were recorded by the coastal videocameras. It has to be noted, that in the case of Poetto, foreshore slope didn't show any significant differentiation and NEPTUNE-EWS proved to provide realistic TWL estimates. However, for other types of beaches where beach slopes show higher variability over time, there is a substantial need for frequent updates of the beach morphology. In comparison to other localized EWSs that similarly integrate hydrodynamic modeling with empirical wave run-up estimates, NEPTUNE-EWS utilizes a different morphological threshold (the berm height), whereas, for example, the system implemented in Emilia-Romagna is based on beach width, expressed as absolute value or distance between the maximum TWL and the buildings located on the backshore (Harley et al., 2012). In addition, the system used for three urban beaches in Barcelona is based on the predicted flood extent, (expressed as a percentage for the whole beach) at times when forecasted Hs exceeds a 2 m threshold (Sanchez-Artus et al., 2025). Future improvements shall involve regular updates of the morphological threshold based on dedicated field surveys. Mediterranean beaches show a marked difference between winter and summer profiles, as in the fair-weather season wave action is moderated. The inclusion of a representative beach morphology is two-fold. A first possibility could involve carrying out a survey at the end of the period of highest wave activity (e.g. in May/June) and one at the end of the fair-weather period (e.g. October). A different possibility could be using all the available surveys to produce a "representative" profile for the winter and one for summer season (e.g. through EOF analysis). Even though calibrated and validated hydrodynamic models provide consistent information on total water levels and can be checked with predefined alert thresholds, these models do not consider hydro-morphodynamic

https://doi.org/10.5194/egusphere-2025-2292
Preprint. Discussion started: 17 June 2025

interactions. Thus, incorporating effective methods for modeling beach hydro-morphodynamics like coupling spectra model with a wave-resolving sediment transport model (for instance SWAN and XBeach) could account for the changing morphology during the event, where beach erosion would change beach characteristics and ultimately the slope with a large control on wave run-up values. Nevertheless, the use of a numerical model like XBeach, would not only require more computational time for model runs, but also computational effort for appropriate calibration of the model parameters, as the default configuration tends to overestimate changes in beach morphology (e.g. Biolchi et al., 2022). This should be based on sedimentological, wind, hydrodynamic, as well as pre- and post-storm topo-bathymetric data. Other approaches like the Bayesian network-based system of Garzon et al. (2023) introduce probabilistic assessments of flood likelihood, whereas NEPTUNE-EWS follows a deterministic approach. Once more data of flooding events becomes available, future improvements may involve incorporating such probabilistic methods or/and deterministic ANNs to enhance forecast reliability under uncertain wave and surge conditions, similar to the approach of Zampato et al., (2016). Finally, it would be interesting to incorporate one or more machine learning algorithms to run in parallel with the use of the same input parameters as an alternative method for TWL forecasting and investigate their predictions against the validated approach of NEPTUNE-EWS.

5. Conclusions

This study presents an early warning system for coastal flooding at Poetto beach. The system integrates wind, waves and sea level forecasts, from widely used databases (ECMWF and CMEMS), whose accuracy has been checked against *in-situ* records. Although slight differences were observed, these are attributed to the spatial offset between the forecasted points and the locations of the *in-situ* measurements. Nevertheless, forecasted data are found to have successfully captured the overall trends. The system provides Total Water Level (TWL) estimates to predict coastal flooding at a local/beach scale. Results showed that forecasted wind, waves and sea level data generally aligned well with the *in-situ* records,

For the case of the intermediate sloped Poetto beach, among the six tested wave run-up parameterizations, the estimates based on the formulae of Stockdon et al. (2006) were found to provide the most realistic results when incorporated into the TWL calculation. In addition, it was critical to include wave-induced processes, such as wave set-up and swash excursion, in TWL estimations. While some studies exclude these components, the results of this work highlight their contribution to achieving more realistic estimations of TWL, particularly in areas characterized by significant wave action, like Poetto beach.

NEPTUNE-EWS proved to be a reliable tool for forecasting coastal flooding, with its predictions aligning well with the monitored overwash/flood events. The system's ability to replicate storm events, particularly during high-energy conditions, underscores its utility in coastal risk management and flood forecasting at a localized/beach scale. The findings point at the need for continuous updates of the morphological threshold. Further improvements that involve effective representation of the nearshore hydro-morphodynamic processes, through the integration of numerical models capable of simulating changes in beach morphology dynamically, are expected to enhance its operational efficiency. Future research should also focus on the incorporation of a module for enhancing the reliability of the downscaled CMEMS and ECMWF forecasts, as well as a parallel

https://doi.org/10.5194/egusphere-2025-2292
Preprint. Discussion started: 17 June 2025

module that employs machine learning algorithms capable of providing accurate TWL forecasts with significantly reduced computational time and effort.

Code Availability. The Copernicus Marine Toolbox (version 2.0.0), integrated into the developed software, is available from Copernicus Marine Service (CMS, 2025). The SWAN model is freely available at https://swanmodel.sourceforge.io. System functions and configuration files developed in this study are available from the corresponding author upon reasonable request.

Data availability. The forecast/re-analysis data used in this study are reported in Table 1. *In-situ* wind and sea level data used for validation are freely accessible through the monitoring network of the Italian Institute for Environmental Protection and Research (ISPRA, 2025). Optical data (frames) recorded by the coastal video monitoring system during overwash/flood events S1 to S6, used for validation of NEPTUNE-EWS forecasts, are archived on the Zenodo platform (10.5281/zenodo.15426775). Retrieved topo-bathymetric and wave data, as well as the full dataset (videos) of the monitored events may be available from the corresponding author upon reasonable request.

Author contribution. *Antonis Chatzipavlis*: Conceptualization, Methodology, Software, Validation, Formal analysis, Investigation, Visualization, Writing (Original Draft). *Daniele Trogu*: Conceptualization, Methodology, Resources, Investigation, Writing (Review & Editing). *Andrea Ruju*: Conceptualization, Methodology, Software, Formal analysis, Investigation, Visualization, Writing (Review & Editing). *Juan Montes*: Methodology, Software, Investigation, Writing (Review & Editing). *Antonio Usai*: Resources, Investigation, Writing (Review & Editing). *Marco Porta*: Resources, Investigation, Writing (Review & Editing). *Giovanni Coco*: Supervision, Methodology, Writing (Review & Editing). *Sandro De Muro*: Supervision, Writing (Review & Editing), Funding acquisition. Paolo Ciavola: Supervision, Methodology, Writing (Review & Editing).

Competing interests. The authors declare that they have no conflict of interest.

Acknowledgements. The authors warmly thank Sardegna Progetta for their assistance during field works. The authors also thank the Sardinia Sea Port Authority, the “Deposito PolNato Marina Militare (Navy PolNato Depot Marina Militare)” of Cape S. Elia–Cagliari and Comando supporto logistico di Cagliari (MARICAGLIARI).

Financial support. This study was carried out within the RETURN Extended Partnership and received funding from the European Union Next-Generation EU (National Recovery and Resilience Plan – NRRP, Mission 4, Component 2, Investment 1.3 – D.D. 1243 2/8/2022, PE0000005). The research has also been funded by Regione Autonoma Sardegna under L.R. 7/2007, “Promozione della ricerca scientifica e dell’innovazione tecnologica in Sardegna” for BEACH and TENDER NEPTUNE projects, directed by Sandro De Muro, University of Cagliari. This study was also produced within the framework of the PHD programme in INNOVATION SCIENCES AND TECHNOLOGIES at the University of Cagliari, Cycle XXXVIII, with the support of a scholarship financed by the Ministerial Decree no. 351 of 9th April 2022, based on the NRRP - funded by the

https://doi.org/10.5194/egusphere-2025-2292
Preprint. Discussion started: 17 June 2025

European Union - NextGenerationEU - Mission 4 "Education and Research", Component 1 "Enhancement of the offer of educational services: from nurseries to universities" - Investment 3.4 "Advanced teaching and university skills".

References

Almar, R., Ranasinghe, R., Bergsma, E.W.J., Diaz, H., Melet, A., Papa, F., Vousdoukas, M., Athanasiou, P., Dada, O., Almeida, L.P., and Kestenare, E.: A global analysis of extreme coastal water levels with implications for potential coastal overtopping, Nat. Commun., 12, 1-9. doi:10.1038/s41467-021-24008-9, 2021.

Aniskiewicz, P., Benedyczak, R., Furmanczyk, K., and Andrzejewski, P.: Validation of Empirical Wave Run-up Formulas to the Polish Baltic Sea Coast, J. Coast. Res., 75, p.10075, 243–247, doi:10.2112/SI75-049.1, 2016.

Ardhuin, F., Rogers, E., Babanin, A.V., Filipot, J.F., Magne, R., Roland, A., Van der Westhuysen, A., Queffeulou, P., Lefevre, J.M., Aouf, L., and Collard, F.: Semiempirical dissipation source functions for wind-wave models: Part I, definition, calibration, and validation, J. Phys. Oceanogr., 51(7), 2131-2150, doi:10.1175/2010JPO4324.1, 2009.

Armaroli, C., Ciavola, P., Perini, L., Calabrese, L., Lorito, S., Valentini, A., and Masina, M.: Critical storm thresholds for significant morphological changes and damage along the Emilia-Romagna coastline, Italy. Geomorphology, 143-144, 34- 51, doi:10.1016/j.geomorph.2011.09.006, 2012.

Asariotis, R., Monioudi, I.N., Mohos Naray, V., Velegrakis, A.F., Vousdoukas, M.I., Mentaschi, L., and Feyen, L.: Climate change and seaports: hazards, impacts and policies and legislation for adaptation. Anthropocene Coasts, 7, p.14, doi:10.1007/s44218-024-00047-9, 2024.

Atkinson, A.L., Power, H.E., Moura, T., Hammond, T., Callaghan, D.P., and Baldock, T.E.: Assessment of runup predictions by empirical models on non-truncated beaches on the south-east Australian coast, Coast. Eng., 119, 15-31, doi:10.1016/j.coastaleng.2016.10.001, 2017.

Bajo, M., and Umgiesser, G.: Storm surge forecast through a combination of dynamic and neural network models. Ocean Model., 33(1-2), 1-9, doi:10.1016/j.ocemod.2009.12.007, 2010.

Bakkensen, L.A., and Barrage, L.: Flood risk belief heterogeneity and coastal home price dynamics: Going under water? *National Bureau of Economic Research (NBER),* p.23854, 30 pp., doi:10.3386/w23854, 2021.

Biolchi, L.G., Unguendoli, S., Bressan, L., Giambastiani, B.M.S., and Valentini, A.: Ensemble technique application to an XBeach-based coastal Early Warning System for the Northwest Adriatic Sea (Emilia-Romagna region, Italy), Coast. Eng., 173, p.104081, doi:10.1016/j.coastaleng.2022.104081, 2022.

Biondo, M., Buosi, C., Trogu, D., Mansfield, H., Vacchi, M., Ibba, A., Porta, M., Ruju, A., and De Muro, S.: Natural vs. Anthropic Influence on the Multidecadal Shoreline Changes of Mediterranean Urban Beaches: Lessons from the Gulf of Cagliari (Sardinia), Water, 12 (12), p.3578, doi:10.3390/w12123578, 2020.

Bujak, D., Ilic, S., Milicevic, Hc., and Carevic, D.: Wave Runup Prediction and Alongshore Variability on a Pocket Gravel Beach under Fetch-Limited Wave Conditions, J. Mar. Sci. Eng., 11(3), p.614, doi:10.3390/jmse11030614, 2023.

https://doi.org/10.5194/egusphere-2025-2292
Preprint. Discussion started: 17 June 2025

Cabrita, P., Montes, J., Duo, E., Brunetta, R., and Ciavola, P.: The Role of Different Total Water Level Definitions in Coastal Flood Modelling on a Low-Elevation Dune System, J. Mar. Sci. Eng., 12, p.1003, doi:10.3390/jmse12061003, 2024.

Caruso, M.F., and Marani, M.: Extreme-Coastal-Water-Level Estimation and Projection: A Comparison of Statistical Methods, Nat. Hazards Earth Syst. Sci., 22, 1109-1128, doi:10.5194/nhess-22-1109-2022, 2022.

Cavaleri, L., Balsamo, G., Beljaars, A., Bertotti, L., Davison, S., Edwards, J., Kanehama, T., and Wedi, N.: ECMWF and UK Met Office Offshore Blowing Winds: Impact of Horizontal Resolution and Coastal Orography, J. Geophys. Res.: Atmospheres, 129(6), 14 pp., doi:10.1029/2023JD039673, 2024.

Ciavola, P., Ferreira, O., Haerens, P., Van Koningsveld, M., and Armaroli C.: Storm impacts along European coastlines. Part 2: lessons learned from the MICORE project, Environ. Sci. Policy, 14, 924-933, doi:10.1016/j.envsci.2011.05.009, 2011.

Chao, W.T., Young, C.C., Hsu, T.W., Liu, W.C., and Liu, C.Y.: Long-lead-time prediction of storm surge using artificial neural networks and effective typhoon parameters: revisit and deeper insight, Water 12(9), p.2394, doi:10.3390/w12092394, 2020.

Clementi, E., Aydogdu, A., Goglio, A.C., Pistoia, J., Escudier, R., Drudi, M., Grandi, A., Mariani, A., Lyubartsev, V., Lecci, R., Cretí, S., Coppini, G., Masina, S., and Pinardi, N.: Mediterranean Sea Physical Analysis and Forecast (CMEMS MED-Currents, EAS6 system) (Version 1) [Data set]. Copernicus Monitoring Environment Marine Service (CMEMS), doi:10.25423/CMCC/MEDSEA_ANALYSISFORECAST_PHY_006_013_EAS8, 2021.

CMS: Quality Information Document for the Mediterranean Sea Physics Analysis and Forecasting Product MEDSEA_ANALYSISFORECAST_PHY_006_013, Copernicus Marine Service, 63 pp., https://catalogue.marine.copernicus.eu/documents/QUID/CMEMS-MED-QUID-006-013.pdf, (last access: 04 March 2025), 2024.

CMS: New Release: Copernicus Marine Toolbox (version 2.0.0), Copernicus Marine Service, https://marine.copernicus.eu/news/new-release-copernicus-marine-toolbox, (last access: 05 March 2025), 2025.

Cohn, N., and Ruggiero, P.: The influence of seasonal to interannual nearshore profile variability on extreme water levels: Modeling wave runup on dissipative beaches, Coast. Eng., 115, 79–92. doi:10.1016/j.coastaleng.2016.01.006, 2016.

Croteau, R., Pacheco, A., and Ferreira, O.: Flood Vulnerability under Sea Level Rise for a Coastal Community Located in a Back-barrier Environment, Portugal, J. Coast. Conserv., 27(28), 16 pp., doi:10.1007/s11852-023-00955-x, 2023.

Dato, J.F., Dinapoli, M.G., D'Onofrio, E.E., and Simionato, C.G.: On water level forecasting using artificial neural networks: the case of the Río de la Plata Estuary, Argentina. Nat. Hazards, 120, 9753-9776. doi:10.1007/s11069-024-06585-2, 2024.

Douglass, S.L.: Estimating extreme values of run-up on beaches, J. Waterway Port Coast. Ocean Eng., 118(2), 220–224, doi:10.1061/(ASCE)0733-950X(1992)118:2(220), 1992.

Del Rio, L., Plomaritis, T.A., Benavente, J., Valladares, M., and Ribera, P.: Establishing Storm Thresholds for the Spanish Gulf of Cádiz. Geomorphology, 143-144, 13-23. doi:10.1016/j.geomorph.2011.04.048, 2012.

https://doi.org/10.5194/egusphere-2025-2292
Preprint. Discussion started: 17 June 2025

De Muro, S., Porta, M., Passarella, M., and Ibba, A.: Geomorphology of four wave-dominated microtidal Mediterranean beach systems with Posidonia oceanica meadow: a case study of the Northern Sardinia coast. J. Maps, 13(2), 74-85. doi:10.1080/17445647.2016.1259593, 2017.

ECMWF, (2025): Atmospheric Model high resolution 15-day forecast (Set I - HRES), European Center for Medium-Range Weather Forecasts, https://.ecmwf.int/en/forecasts/datasets/set-i, (last access: 12 April 2025), 2025.

EMODnet Bathymetry Consortium: EMODnet Digital Bathymetry (DTM 2024), doi:10.12770/cf51df64-56f9-4a99-b1aa-36b8d7b743a1, (last access: 12 December 2024), 2024.

Garzon, J.L., Ferreira, O., Zozimo, A.C., Fortes, C.J.E.M., Ferreira, A.M., Pinheiro, L.V., and Reis, M.T.: Development of a Bayesian networks-based early warning system for wave-induced flooding, Int. J. Disaster Risk Reduct., 96, p.103931, doi:10.1016/j.ijdrr.2023.103931, 2023.

Gomes da Silva, P., Coco, G., Garnier, R., and Klein, A.H.F.: On the prediction of runup, setup and swash on beaches, Earth Sci. Rev., 204, p.103148, 22 pp., doi:10.1016/j.earscirev.2020.103148, 2020.

Haiden, T., Janousek, M., Vitart, F., Tanguy, M., Prates, F. and Chevallier, M.: Evaluation of ECMWF forecasts, ECMWF Technical Report, 62 pp., https://www.ecmwf.int/sites/default/files/elibrary/092024/81582-evaluation-of-ecmwf-forecasts_0.pdf, (last access 21 02 2025), 2024.

Harley, M.D., Valentini, A., Armaroli, C., Ciavola, P., Perini, L., Calabrese, L., and Marucci, F.: An early warning system for the on-line prediction of coastal storm risk on the Italian coastline, Coast. Eng. Proc., 1(33), 11 pp., doi:10.9753/icce.v33.management.77, 2012.

Hashemi, M.R., Spaulding, M.L., Shaw, A., Farhadi, H., and Lewis, M.: An efficient artificial intelligence model for prediction of tropical storm surge. Nat. Hazards, 82(1), 471-491. doi:10.1007/s11069-016-2193-4, 2016.

Hasselmann, K., Barnett, T., Bouws, E., Carlson, H., Cartwright, D., Enke, K., Ewing, J.A., Gienapp, H., Hasselmann, D.E., Kruseman, P., Meerburg, A., Müller, P., Olbers, D.J., Richter, K., Sell, W., and Walden, H.: Measurements of wind-wave growth and swell decay during the Joint North Sea Wave Project (JONSWAP). Deut. Hydrograf. Z., 8(12), 1-95, 1973.

Hauer, M.E., Evans, J. M., and Mishra D.R.: Millions projected to be at risk from sea-level rise in the continental United States, Nat. Clim. Chang., 6, 691-695. doi:10.1038/nclimate2961, 2016.

Hersbach, H., Bell, B., Berrisford, P., Hirahara, S., Horányi, A., Muñoz-Sabater, J., et al.: The ERA5 global reanalysis. Q. J. R. Meteorol. Soc., 146(730), 1999–2049, doi:10.1002/qj.3803, 2020.

Holman, R.A.: Extreme value statistics for wave run-up on a natural beach, Coast. Eng., 9, 527-544, doi:10.1016/0378-3839(86)90002-5, 1986.

Hunt I.A.: Design of seawalls and breakwaters, J. Waterw. Harb. Div. ASCE, 85 (WW3), 123-152, doi:10.1061/JWHEAU.0000129, 1959.

IPCC: Climate Change 2023: Synthesis Report. Contribution of Working Groups I, II and III to the Sixth Assessment Report of the Intergovernmental Panel on Climate Change [Core Writing Team, Lee, H.-O. (eds.)], IPCC, Geneva, Switzerland, 202 pp. doi:10.59327/IPCC/AR6-9789291691647, 2023.

https://doi.org/10.5194/egusphere-2025-2292
Preprint. Discussion started: 17 June 2025

ISPRA: Tide Gauge Network - Cagliari Monitoring Station, Istituto Superiore per la Protezione e la Ricerca Ambientale, https://www.mareografico.it/?session=0S97946769682PJFG83R68&syslng=ita&sysmen=2&sysind=13&syssub=0&sysfnt=0&code=STAZ&idst=1I, (last access: 14 March 2025), 2025.

Irazoqui Apecechea, M., Melet, A. and Armaroli, C.: Towards a Pan-European Coastal Flood Awareness System: Skill of Extreme Sea-Level Forecasts from the Copernicus Marine Service, Front. Mar. Sci., 9, p.1091844, doi:10.3389/fmars.2022.1091844, 2023.

Iribarren, C.R., and Nogales, C.: Protection des ports, Proceedings of the XVIIth International Navigation Congress, Lisbon, Portugal, Section II, Communication, 4, 31-80, 1949.

Jelesnianski, C.P., Chen, J., and Shaffer, W.A.: SLOSH: Sea, Lake, and Overland Surges from Hurricanes, National Oceanic and Atmospheric Administration, Technical Report NWS 48, https://repository.library.noaa.gov/view/noaa/7235/noaa_7235_DS1.pdf, (last access: 28 July 2024), 1992.

Jevrejeva, S., Jackson, L.P., Riva, R.E., Grinsted, A., and Moore, J.C.: Coastal sea level rise with warming above 2°C, Proc. Natl. Acad. Sci. U.S.A., 113(47), 13342-13347, doi:10.1073/pnas.1605312113, 2016.

Jimenez, J., Ciavola, P., Balouin, Y., Armaroli, C., Bosom, E., and Gervais, M.: Geomorphic Coastal Vulnerability to Storms in Microtidal Fetch-Limited Environments: Application to NW Mediterranean and N Adriatic Seas, J. Coast. Res., 56, 1641–1645, 2009.

Klonaris, G.Th., Memos, C.D., and Karambas, Th.V.: A Boussinesq-type model including wave-breaking terms in both continuity and momentum equations, Ocean Eng., 57, 128-140. doi:10.1016/j.oceaneng.2012.08.007, 2013.

Korres, G., Ravdas, M., Zacharioudaki, A., Denaxa, D., and Sotiropoulou, M.: Mediterranean Sea Waves Reanalysis (CMEMS Med-Waves, MedWAM3 system) (Version 1) [Data set]. Copernicus Monitoring Environment Marine Service, doi:10.25423/CMCC/MEDSEA_MULTIYEAR_WAV_006_012, (last access: 12 February 2025), 2021.

Korres, G., Oikonomou, C., Denaxa, D., and Sotiropoulou, M.: Mediterranean Sea Waves Analysis and Forecast (Copernicus Marine Service MED-Waves, MEDWAM4 system) (Version 1) [Data set], Copernicus Marine Service, doi:10.25423/CMCC/MEDSEA_ANALYSISFORECAST_WAV_006_017_MEDWAM4, (last access: 12 February 2025), 2023.

Le Gal, M., Fernandez-Montblanc, T., Duo, E., Montes Perez, J., Cabrita, P., Souto Ceccon, P., Gastal, V., Ciavola, P., and Armaroli, C.: A New European Coastal Flood Database for Low-Medium Intensity Events, Nat. Hazards Earth Syst. Sci., 23(11), 3585-3602, doi:10.5194/nhess-23-3585-2023, 2023.

Monioudi, I.N., Asariotis, R., Becker, A., Bhat, C., Dowding-Gooden, D., Esteban, M., Feyen, L., Mentaschi, L., Nikolaou, A., Nurse, L., Phillips, W., Smith, D.A.Y., Satoh, M., Trotz, U.O'D., Velegrakis, A. F., Voukouvalas, E., Vousdoukas, M.I., and Witkop, R.: Climate change impacts on critical international transportation assets of Caribbean Small Island Developing States (SIDS): the case of Jamaica and Saint Lucia, Reg. Environ. Change, 18, 2211–2225. doi:10.1007/s10113-018-1360-4, 2018.

https://doi.org/10.5194/egusphere-2025-2292
Preprint. Discussion started: 17 June 2025

Murfin, J., and Spiegel, M.: Is the risk of sea level rise capitalized in residential real estate?, Rev. Financ. Stud., 33(3), 1217-1255. doi:10.1093/rfs/hhz134, 2020.

Naeini, S.S., and Snaiki, R.: A physics-informed machine learning model for time-dependent wave runup prediction, Ocean Eng., 295, p.116986, doi:10.1016/j.oceaneng.2024.116986, 2024.

Neumann, B., Vafeidis, A.T., Zimmermann, J., and Nicholls, R.J.: Future coastal population growth and exposure to sea-level rise and coastal flooding - a global assessment, PLoSONE, 10(3), p.e0118571, doi:10.1371/journal.pone.0118571, 2015a

Neumann, J.E., Price, J., Chinowsky, P., Wright, L., Ludwig, L., Streeter, R., Jones, R., Smith, J.B., Perkins, W., Jantarasami, L., and Martinich, J.: Climate change risks to US infrastructure: impacts on roads, bridges, coastal development, and urban drainage, *Clim. Change*, 131, 97-109. doi:10.1007/s10584-013-1037-4, 2015b.

Nicholls, R.J., Hinkel, J., Lincke, D., and van der Pol, T.: Global investment costs for coastal defense through the 21st century". *The World Bank*, p.8745, 64 pp., doi:10.1596/1813-9450-8745, 2019.

Nielsen, P., and Hanslow, D.J.: Wave run-up distributions on natural beaches, J. Coast. Res., 7(4), 1139-1152, 1991.

Oikonomou, C., Denaxa, D., and Korres, G.: Quality Information Document for Mediterranean Production Centre, product: MEDSEA_ANALYSISFORECAST_WAV_006_017, Copernicus Marine Service, 39 pp. https://catalogue.marine.copernicus.eu/documents/QUID/CMEMS-MED-QUID-006-017.pdf, (last access: 13 February 2025), 2023.

Paprotny, D., Andrzejewski, P., Terefenko, P., and Furmanczyk, K.: Application of Empirical Wave Run-Up Formulas to the Polish Baltic Sea Coast, PLoSONE, 9(8), p.e105437, 8 pp., doi:10.1371/journal.pone.0105437, 2014.

Perez-Gomez, B., Garcia-Leon, M., Garcia-Valdecasas, J., Clementi, E., Mosso Aranda, C., Perez-Rubio, S., Masina, S., Coppini, G., Molina-Sanchez, R., Munoz-Cubillo, A., Garcia Fletcher, A., Sanchez Gonzalez, J.F., Sanchez-Arcilla, A., and Alvarez Fanjul, E.: Understanding Sea Level Processes During Western Mediterranean Storm Gloria, Front. Mar. Sci., 8, p.647437, 1-22, doi:10.3389/fmars.2021.647437, 2021.

Poate, T.G., McCall, R., and Masselink, G.: A new parameterisation for runup on gravel beaches. Coast/ Eng., 117, 176-190. doi:10.1016/j.coastaleng.2016.08.003, 2016.

Pugh, D.T.: Tides, Surges, and Mean Sea-Level: A Handbook for Engineers and Scientists. John Wiley and Sons Ltd., Hoboken, New York, USA, 472 pp., ISBN: 047191505X., 1987.

Roelvink, D., Reneirs, A., van Dongeren, A., van Thiel de Vries, J., McCall, R., and Lescinsky, J.: Modeling storm impacts on beaches, dunes and barrier islands, Coast. Eng., 56, 1133-1152. doi:10.1016/j.coastaleng.2009.08.006, 2009.

Ruju, A., Passarella, M., Trogu, D., Buosi, C., Ibba, A., De Muro, S.: An operational wave system within the monitoring program of a mediterranean beach, J. Mar Sci. Eng. 7(2):32, doi:10.3390/jmse7020032, 2019.

Ruju, A., Buosi, C., Coco G., Porta M., Trogu, D.; Ibba, A. and De Muro, S. (2022) Ecosystem services of reed and seagrass debris on a urban Mediterranean beach (Poetto, Italy). Estuar. Coast. Shelf Sci., 271, p.107862, doi:10.1016/j.ecss.2022.107862, 2022.

https://doi.org/10.5194/egusphere-2025-2292
Preprint. Discussion started: 17 June 2025

Ruju, A., and Viola, F.:. An assessment of the impact of boundary conditions in dynamical downscaling techniques for fetch-limited waves. Coast. Eng. J., 66(4), 637–658. doi:10.1080/21664250.2024.2399393, 2024.

Ruggiero, P., Holman, R.A. and Beach, R.A.: Wave run-up on a high-energy dissipative beach, J. Geophys. Res., 109 (C6), p.C06025, 12 pp. doi:10.1029/2003JC002160, 2004.

Rulent, J., Calafat, F.M., Banks, C.J., Bricheno, L.M., Gommenginger, C., Green, J.A.M., Haigh, I.D., Lewis, H., and Martin, A.C.H.: Comparing Water Level Estimation in Coastal and Shelf Seas from Satellite Altimetry and Numerical Models. Front. Mar. Sci., 7, p.549467. doi:10.3389/fmars.2020.549467, 2020.

Sanchez-Arcilla, A., Gomez-Aguar, J., Egozcue, J.J., Ortego, M.I., Galiatsatou, P., and Prinos, P.: Extremes from scarce data. The role of Bayesian and scaling techniques in reducing uncertainty, J. Hydraul. Res., 46 (2), 224-234. doi:10.1080/00221686.2008.9521956, 2008.

Sanchez-Artus, X., Gracia, V., Espino, M., Grifoll, M., Simarro, G., Guillen, J., Gonzalez, M., and Sanchez-Arcilla A.: Operational hydrodynamic service as a tool for coastal flood assessment., Ocean Sci., 21, 749-766, doi:10.5194/os-21-749-2025, 2025.

Sardegna Geoportale, WMS Service - Regione Sardegna. https://webgis.regione.sardegna.it/geoserverraster/ows?service=WMS&request=GetCapabilities (last access, 05 May 2024), 2024.

Senechal, N., Coco, G., Bryan, K.R., and Holman, R.A.: Wave runup during extreme storm conditions. Journal of Geophysical Research: Oceans, 116 116(C7), p.C07032, 243–247. doi:10.1029/2010JC006819, 2011.

Stephens, E., and Cloke, H.: Improving flood forecasts for better flood preparedness in the UK (and beyond), Geogr. J., 180(4), 310-316. doi:10.1111/geoj.12103, 2014.

Stockdon, H.F., Holman, R.A., Howd, P.A., and Sallenger, J.A.H.: Empirical parameterization of setup, swash, and runup, Coast. Eng., 53(7), 573-588. doi:10.1016/j.coastaleng.2005.12.005, 2006.

Stokes, K., Poate, T. Masselink, G., King, E., Saulter, A., and Ely, N.: Forecasting coastal overtopping at engineered and naturally defended coastlines, Coast. Eng., 164, p.103827, doi: 10.1016/j.coastaleng.2020.103827, 2021.

Strazzera, E., Cherchi, E., and Ferrini, S.: A choice modelling approach for assessment of use and quasi option value in urban planning for areas of environmental interest. Fondazione Eni Enrico Mattei, p.NDL63.2008, 32 pp. doi:10.22004/ag.econ.42903, 2008.

Suanez, S., Blaise, E., Cancouet, R., and Floch, F.: Empirical Parameterization of Wave Runup and Dune Erosion during Storm Conditions on a Natural Macrotidal Beach Serge, J. Coast. Res., 75, 932-936. doi:10.2112/SI75-187.1, 2016.

Trogu, D., Simeone, S., Ruju, A., Porta, M., Ibba, A., and De Muro S.: A Four-Year Video Monitoring Analysis of the Posidonia oceanica Banquette Dynamic: A Case Study from an Urban Microtidal Mediterranean Beach (Poetto Beach, Southern Sardinia, Italy), J. Mar. Sci. Eng., 11(12), p.2376, doi:10.3390/jmse11122376, 2023.

Trogu, D., Simeone, S., Usai, A., Porta, M., and De Muro, S.: On the role of wood and seagrass rests in coastal flooding events in Mediterranean microtidal beaches. J. Mar. Sci. Eng., SI no. 113, 115-119. doi:10.2112/JCR-SI113-023.1, 2024.

https://doi.org/10.5194/egusphere-2025-2292
Preprint. Discussion started: 17 June 2025

UNCTAD: Climate change impacts on coastal transport infrastructure in the Caribbean: enhancing the adaptive capacity of Small Island Developing States (SIDS), Saint Lucia: A case study. United Nations Conference on Trade and Development (UNCTAD), UNDA project 1415O, 136 pp., https://unctad.org/system/files/official-document/dtltlb2018d3_en.pdf, (last access: 27 July 2024), 2018.

USACE: Shore Protection Manual, United States Army Corps of Engineers - Coastal Engineering Research Center, United States Washington, DC, USA, 1984.

Vousdoukas, M.I., Velegrakis, A.F, Dimou, K., Zervakis, V., and Conley, D.C.: Wave run-up observations in microtidal, sediment-starved beaches of the Eastern Mediterranean. J. Mar. Syst., 78, 537-547. doi:10.1016/j.jmarsys.2009.01.004, 2009.

Vousdoukas, M.I., Wziatek, D., and Almeida, L.P.: Coastal vulnerability assessment based on video wave run-up observations at a mesotidal, steep-sloped beach. Ocean Dyn., 62, 123–137. doi:10.1007/s10236-011-0480-x, 2012.

Vousdoukas, M.I., Voukouvalas, E., Mentaschi, L., Dottori, F., Giardino, A., Bouziotas, D., Bianchi, A., Salamon, P. and Feyen, L.: Developments in Large-Scale Coastal Flood Hazard Mapping. Nat. Hazards Earth Syst. Sci., 16, 1841–1853, doi:10.5194/nhess-16-1841-2016, 2016.

Vousdoukas, M.I., Mentaschi, L., Voukouvalas, E., Bianchi, A., Dottori, F., and Feyen, L.: Climatic and socioeconomic controls of future coastal flood risk in Europe, Nat. Clim. Chang., 8, 776–780, doi:10.1038/s41558-018-0260-4, 2018a.

Vousdoukas, M.I., Mentaschi, L., Voukouvalas, E.; Verlaan, M., Jevrejeva, S., Jackson, L.P., and Feyen, L.: Global Probabilistic Projections of Extreme Sea Levels Show Intensification of Coastal Flood Hazard, Nat. Commun., 9, p.2360, doi:10.1038/s41467-018-04692-w, 2018b.

Vousdoukas, M., Mentaschi, L., Mongelli, I., Ciscar Martinez, J., Hinkel, J., Ward, P., Gosling, S., and Feyen, L.: Adapting to rising coastal flood risk in the EU under climate change, Publications Office of the European Union, Luxembourg, JRC118512, ISBN 978-92-76-12990-5, doi:10.2760/456870, 2020.

Wang, Q., Chen, J., and Hu, K.: Storm surge prediction for Louisiana coast using artificial neural networks. In: Hirose, A., Ozawa, S., Doya, K., Ikeda, K., Lee, M., Liu, D. (eds), Neural Information Processing, ICONIP 2016, Lecture Notes in Computer Science, Springer, Cham, Switzerland, 9949, 396-405. doi:10.1007/978-3-319-46675-0_43, 2016.

Wang, W., and Yuan, H.: A tidal level prediction approach based on BP neural network and cubic B-spline curve with knot insertion algorithm, Math. Probl. Eng., 2018(1), p.9835079, doi:10.1155/2018/9835079, 2018.

Xiao, C., Zhang, K., and Shen, J.: CEST: A Three-Dimensional Coastal and Estuarine Storm Tide Model. Miami, Florida: International Hurricane Research Center, Florida International University, 20 pp., 2006.

Zampato, L., Bajo, M., Canestrelli, P., and Umgiesser, G.: Storm surge modelling in Venice: two years of operational results, J. Oper. Oceanogr., 9, 46–57, doi:10.1080/1755876x.2015.1118804, 2016.

Zijlema, M., and van der Westhuysen, A.J.: On convergence behaviour and numerical accuracy in stationary SWAN simulations of nearshore wind wave spectra, Coast. Eng., 52(3), 237–256. doi:10.1016/j.coastaleng.2004.12.006, 2005.

https://doi.org/10.5194/egusphere-2025-2292
Preprint. Discussion started: 17 June 2025

Zijlema, M., Stelling, G.S., and Smit, P.B.: SWASH: An operational public domain code for simulating wave fields and rapidly varied flows in coastal waters, Coast. Eng., 58(10), 992-1012. doi:10.1016/j.coastaleng.2011.05.015, 2011.